

CHIRAL TRANSITION METAL CLUSTERS

SYNTHESIS AND NMR STUDIES
OF CHIRAL TRANSITION
METAL CLUSTERS

by

DEBBIE TANIA CLARK, B.Sc.

A Thesis

Submitted to the Faculty of Graduate Studies
In Partial Fulfilment of the Requirements
for the Degree
Master of Science

McMaster University

August, 1988

(c)Copyright by Debbie Tania Clark 1988.

MASTER OF SCIENCE (1988)
(Chemistry)

McMaster University
Hamilton, Ontario

TITLE: Synthesis and NMR Studies of Chiral Transition
Metal Clusters

AUTHOR: Debbie Tania Clark, B.Sc. (McMaster University)

SUPERVISOR: Dr. M. J. McGlinchey

NUMBER OF PAGES: xii, 85

Abstract

A series of chiral transition metal clusters of the type $MCo_2(CO)_6C-CO_2R$, where $M = Co(CO)_3$, $(C_5H_5)Mo(CO)_2$, $(i-Pr-C_5H_4)Mo(CO)_2$ or $(indenyl)Mo(CO)_2$ and $R =$ menthyl or *exo*-bornyl have been synthesized and characterized using FAB mass spectrometry and high field NMR techniques. The isopropyl Cp and the indenyl ligands served as NMR probes to detect the chirality created by the incorporation of the terpenoidal capping group.

The tricobalt clusters were treated with the bidentate ligands arphos, $Ph_2AsCH_2CH_2PPh_2$ and diphos, $Ph_2PCH_2CH_2PPh_2$. Treatment with arphos yields a pair of diastereomers which are interconverted via the migration of the Ph_2As terminus of the arphos ligand from one cobalt vertex to another. This fluxionality was monitored by variable-temperature ^{31}P NMR spectroscopy. The diphos cluster is not a fluxional molecule. However, the $Co(CO)_2P$ vertices are diastereotopic and give two signals in the ^{31}P NMR. Thus, diphos serves as a convenient probe for chirality.

In the case where $M = Co(CO)_3$, the two remaining cobalt vertices are diastereotopic and are, in principle, not equally susceptible to attack by an incoming ligand. To test for chiral discrimination, these molecules have

been treated with several different phosphines. If the reaction were to proceed with any degree of selectivity, the ^{31}P NMR spectrum ought to show resonances of unequal intensity. Such results have been obtained when a bulky phosphine, such as tricyclohexylphosphine, has been employed.

ACKNOWLEDGEMENTS

There are so many people that I wish to thank for their guidance and friendship during my years at McMaster.

First and foremost, I would like to thank my research supervisor, Dr. M. J. McGlinchey, for his encouragement and advice throughout this project. No matter how busy he was, he always had time to listen to me and to make helpful suggestions. I am also grateful to him for the many "non-chemistry" talks we had. He has not only been an enthusiastic and dedicated supervisor, but also a very good friend.

I have received much guidance during my years at this school. Dr. Willie Leigh gave me my first opportunity to work in a lab and he taught me a lot. Dr. Brian McCarry taught me to do organic chemistry (and to like it, too!). Dr. Michael Brook has saved me countless hours in the lab by showing me how to run a flash column. I don't know how I ever got by without this technique. Dr. Michael Mlekuz made me an organometallic chemist. His patience and direction will not be forgotten. I have been very fortunate to have such good teachers.

I wish to thank everyone in the mass spectrometry and NMR facilities: Dr. R. Smith, F. A. Ramelan, Jack Chan, Brian Sayer, Dr. D. Hughes and Ian Thompson. Their importance to my project is clearly obvious in this thesis.

I express my gratitude to everyone with whom I have worked in 357: Richard, Karen, Michael, Bavani, Ian, Jan, Kris, Andreas and Tim. Their friendship means a lot to me. Besides friendship, they have also helped me in my research. I thank Richard, Karen and Michael for the many spectra that they have run for me. I would also like to thank Michael for printing this thesis - I never would have figured it out alone. More importantly, I would like to thank him for being such a good friend to me over the past few years. I am especially grateful to Bavani for giving me a place to stay during my last months in Hamilton. She has been a constant and true friend.

I thank the many, many friends whom I have made here at Mac for all of the good times they have made possible. (You know who you are.)

Finally, I am forever grateful to my parents and family whose love and support mean everything to me. I especially want to thank my husband Brady. His love and understanding have helped me through many a difficult time.

TABLE OF CONTENTS

	<u>PAGE</u>
CHAPTER 1: INTRODUCTION	1
1.1 General	1
1.2 Applications to catalysis	4
1.3 The importance of developing chiral clusters	8
1.4 Routes to developing chiral clusters	9
1.5 Statement of problem	13
CHAPTER 2: PROBES FOR CHIRALITY	14
2.1 Concepts of chirality	14
2.2 Chiral substituents	19
2.3 NMR probes for chirality	21
2.4 Synthesis and characterization of the molybdenum dimers	24
2.5 Results	27
2.6 Further study with the indenyl probe	29
CHAPTER 3: REACTIONS OF CHIRAL CLUSTERS WITH BIDENTATE LIGANDS	31
3.1 Incorporation of the diphos ligand	31
3.2 Incorporation of the arphos ligand	32
3.3 Computer modelling of these systems	37
3.4 Related work in this area	41
3.5 Characterization of the chiral clusters	43

	<u>PAGE</u>
CHAPTER 4: REACTIONS OF CHIRAL MIXED METAL CLUSTERS WITH MONOPHOSPHINES	46
4.1 Introduction	46
4.2 Reactions of monophosphines with $\text{Co}_2(\text{CO})_6\text{MoCp}(\text{CO})_2\text{CCO}_2\text{menthyl}$	51
4.3 Reactions of monophosphines with $\text{Co}_2(\text{CO})_6\text{MoCp}(\text{CO})_2\text{CCO}_2\text{exo-bornyl}$	54
4.4 Characterization of the phosphine substituted clusters	56
4.5 Preparation of a chiral phosphine, $\text{PPh}_2(\text{neomenthyl})$	56
4.6 Treatment of a chiral mixed metal cluster with a chiral phosphine	59
4.7 Related work in this area	59
4.8 Conclusion	62
CHAPTER 5: EXPERIMENTAL	63
5.1 General spectroscopic techniques	63
5.2 General procedures	63
5.3 Experimental procedures	64
5.4 Numbering system	80
REFERENCES	81

LIST OF FIGURES

	<u>PAGE</u>
1. A chiral substituted ethane molecule and its Newman projection.	14
2. A chiral substituted ethane molecule depicting diastereotopic protons, H ₁ and H ₂ .	15
3. Equilibration of the methylene proton environments via racemization of the system.	16
4. Analogous transition metal systems.	18
i) a chiral tricobalt cluster	
ii) a chiral mixed metal cluster in which the two cobalt nuclei are diastereotopic.	
5. Incorporation of a bidentate ligand into a chiral tricobalt cluster renders the cobalt vertices diastereotopic.	17
6. Variable temperature 250 MHz ¹ H NMR spectra of the methyl region of Co ₃ (CO) ₇ (arphos)C-CO ₂ CHMe ₂ , 4.	22
7. High mass region of the FAB mass spectrum of [(C ₅ H ₄ -CHMe ₂)Mo(CO) ₃] ₂ .	26
8. a) Section of the 62.8 MHz ¹³ C spectrum of [(C ₉ H ₇)Mo(CO) ₃] ₂ , 21.	28

	<u>PAGE</u>
8. b) Section of the 125.7 MHz ^{13}C spectrum of $\text{Co}_2(\text{CO})_6\text{Mo}(\text{CO})_2(\text{C}_9\text{H}_7)\text{CCO}_2\text{menthyl}$, 23, showing the splitting of the indenyl five-membered ring carbons, C(1) and C(3).	28
9. Section of the 125.7 MHz ^{13}C NMR spectrum of the diastereomers of $\text{Co}_2(\text{CO})_4(\text{arphos})\text{Mo}(\text{CO})_2(\text{C}_9\text{H}_7)\text{CCO}_2\text{menthyl}$, 24 and 25, showing the further splitting of the indenyl five-membered ring carbons, C(1), C(2) and C(3).	30
10. 101.2 MHz variable temperature ^{31}P NMR spectra of $\text{Co}_3(\text{CO})_7(\text{diphos})\text{CCO}_2\text{menthyl}$, 28, showing clear differentiation of the diastereotopic phosphorus nuclei.	33
11. 101.2 MHz variable temperature ^{31}P NMR spectra of $\text{Co}_3(\text{CO})_7(\text{arphos})\text{CCO}_2\text{menthyl}$, showing a slow interconversion of the diastereomers 29a and 29b at low temperature.	36
12. 101.2 MHz variable temperature ^{31}P NMR spectra of $\text{Co}_3(\text{CO})_7(\text{arphos})\text{CCO}_2\text{exo-bornyl}$, showing the slow interconversion of the diastereomers 30a and 30b at low temperature.	38
13. Chem-X model of $\text{Co}_3(\text{CO})_7(\text{arphos})\text{CCO}_2\text{CHMe}_2$, 4.	40
14. Chem-X model of $\text{Co}_3(\text{CO})_7(\text{arphos})\text{CCO}_2\text{menthyl}$, 29.	40

	<u>PAGE</u>
15. Chem-X model of the tricobalt ether cluster, Co ₃ (CO) ₇ (arphos)C-O-menthyl, 32.	42
16. 500 MHz ¹ H NMR spectra (in CD ₂ Cl ₂) of a) menthol, b) menthyl trichloroacetate, and c) Co ₃ (CO) ₇ - (arphos)CCO ₂ menthyl, 29.	44
17. 500 MHz two-dimensional ¹ H- ¹ H COSY NMR spectrum of Co ₃ (CO) ₇ (arphos)CCO ₂ menthyl, 29.	45
18. 202.4 MHz ³¹ P NMR spectrum of Co ₂ (CO) ₅ [P(OMe) ₃]- MoCp(CO) ₂ CCO ₂ menthyl, 37, showing the ≈ 1 : 1 ratio of diastereomers.	52
19. 202.4 MHz ³¹ P NMR spectrum of Co ₂ (CO) ₅ [P(C ₆ H ₁₁) ₃]- MoCp(CO) ₂ CCO ₂ menthyl, 37, showing the ≈ 1 : 1 ratio of diastereomers.	52
20. High mass region of the FAB mass spectrum of Co ₂ (CO) ₅ [P(OMe) ₃]MoCp(CO) ₂ CCO ₂ <i>exo</i> -bornyl, 39. The peak at <i>m/z</i> 794 corresponds to the M ⁺ ion.	57

LIST OF SCHEMES

	<u>PAGE</u>
1. Hydroformylation of an alkene to produce a straight chain aldehyde, catalyzed by <i>trans</i> -[RhH(CO)(PPh ₃) ₃].	6
2. Synthesis of Co ₃ (CO) ₉ C-O-menthyl, 31.	41
3. Preparation of (+) Neomenthyldiphenylphosphine, 41.	58

LIST OF TABLES

1. Effect of σ -bonding, π -bonding and steric interference on the stability of the metal-phosphorus bond.	49
2. Cone angles for some common phosphines.	50

CHAPTER ONE : INTRODUCTION

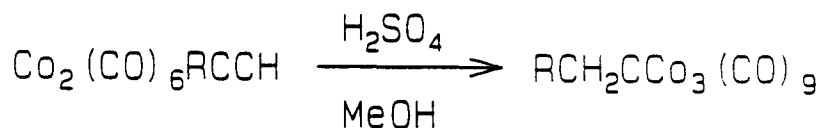
1.1 General

The past twenty years have shown many significant advances in transition metal cluster chemistry.¹ Metal clusters are not only structurally interesting molecules, but also exhibit catalytic potential. It is this possible application to catalysis that has made cluster chemistry such an active area of research.²

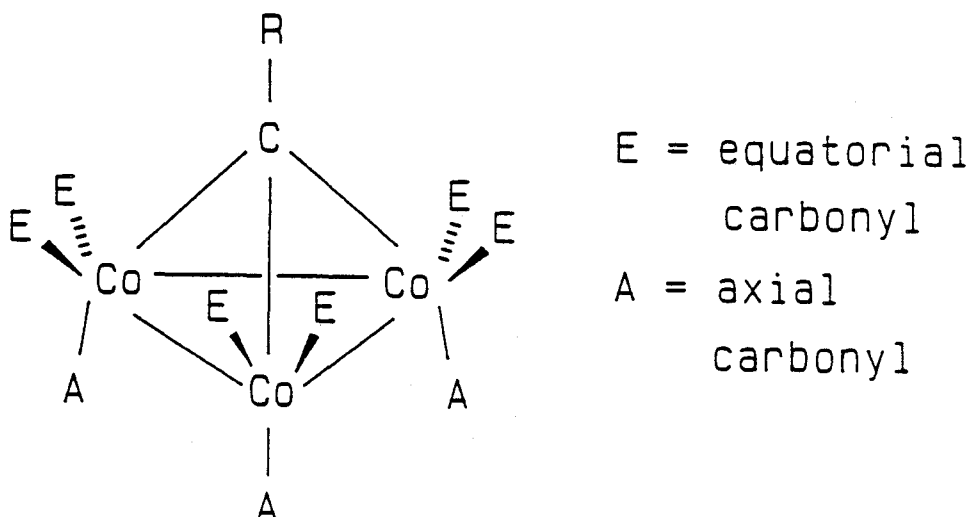
Cotton has described the metal cluster as a group of two or more metal atoms in which there are substantial and direct bonds between the metal atoms.³ The cluster framework can also contain atoms other than metals. These include oxygen, phosphorus, nitrogen, carbon and sulfur.

Transition metal carbonyls make up an entire class of cluster compounds.⁴ These clusters are based on the formula $M_x(CO)_y$, where $x = 2-38$, but can also contain ligands such as phosphines, olefins, hydrides and alkyls. The metal atoms in these clusters possess very low oxidation states, viz. oxidation states of zero or negative values.

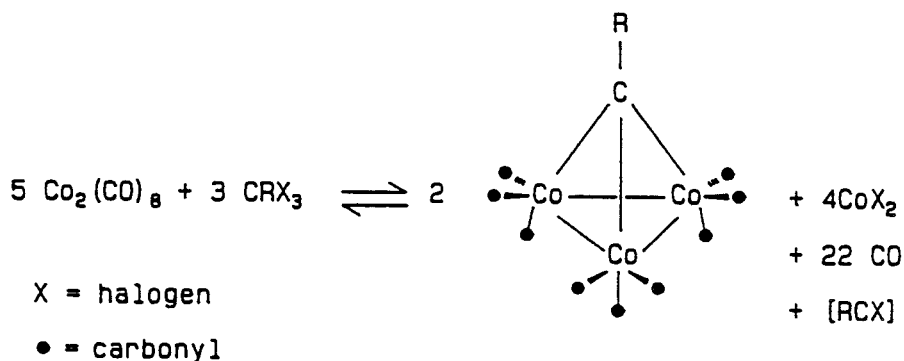
The first methynyltricobalt enneacarbonyl, $\text{CH}_3\text{-CCo}_3(\text{CO})_9$ was prepared serendipitously in 1958 by the reaction of the acetylene complex $\text{Co}_2(\text{CO})_6(\text{HC}\equiv\text{CH})$ with sulfuric acid.⁵ The mechanistic details of this rearrangement remain obscure today but it is established that it only occurs for terminal alkynes.



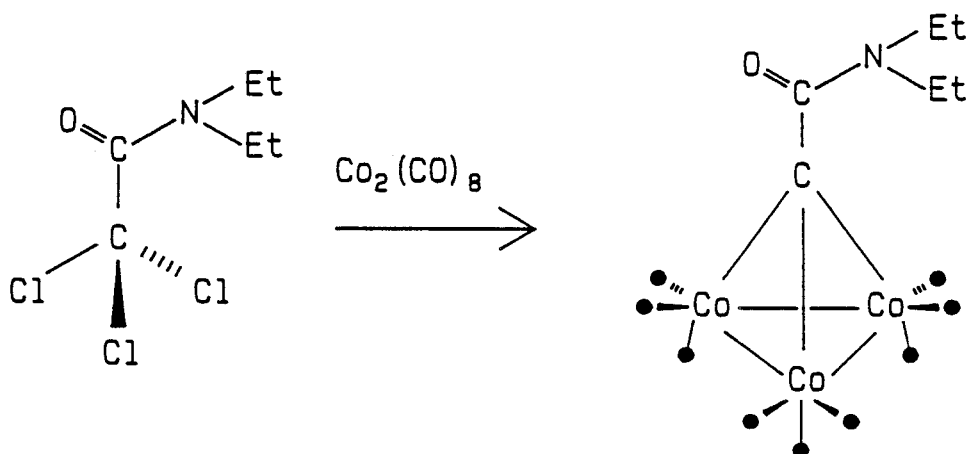
In 1966, the structure of the product was determined by X-ray diffraction.⁶ The three cobalt atoms form a triangular plane with the C-R unit as a capping group. Each cobalt is bonded to three carbonyl groups, two of which are equatorial, and one which is axial. The axial carbonyls point up toward the top of the cluster in a picket fence arrangement around the metal vertices. The significance of this steric factor will become apparent.

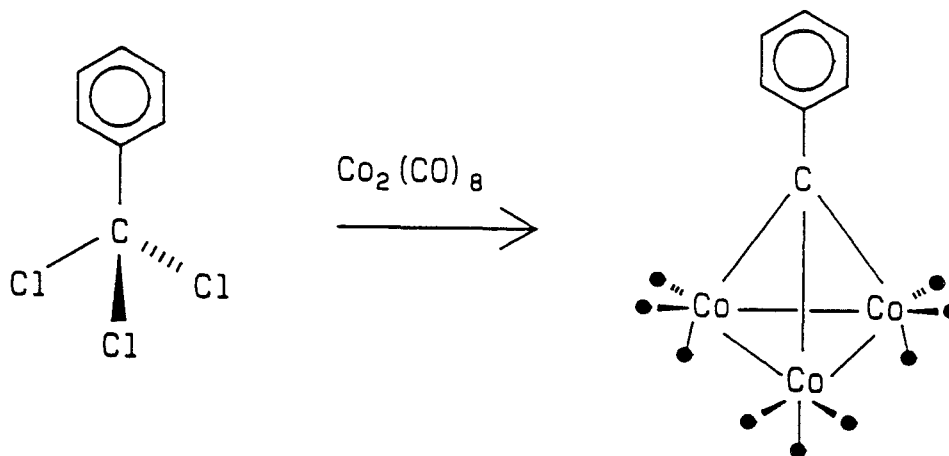


In 1961, a more general route to the synthesis of tricobalt clusters was discovered.⁷ α,α,α -Trihalo compounds were treated with cobalt octacarbonyl to yield the desired cluster species.



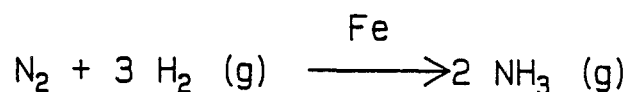
Using this method of preparation, a wider variety of apical groups could be built into the metal cluster. Examples of these are as follows:⁸





1.2 Applications to catalysis

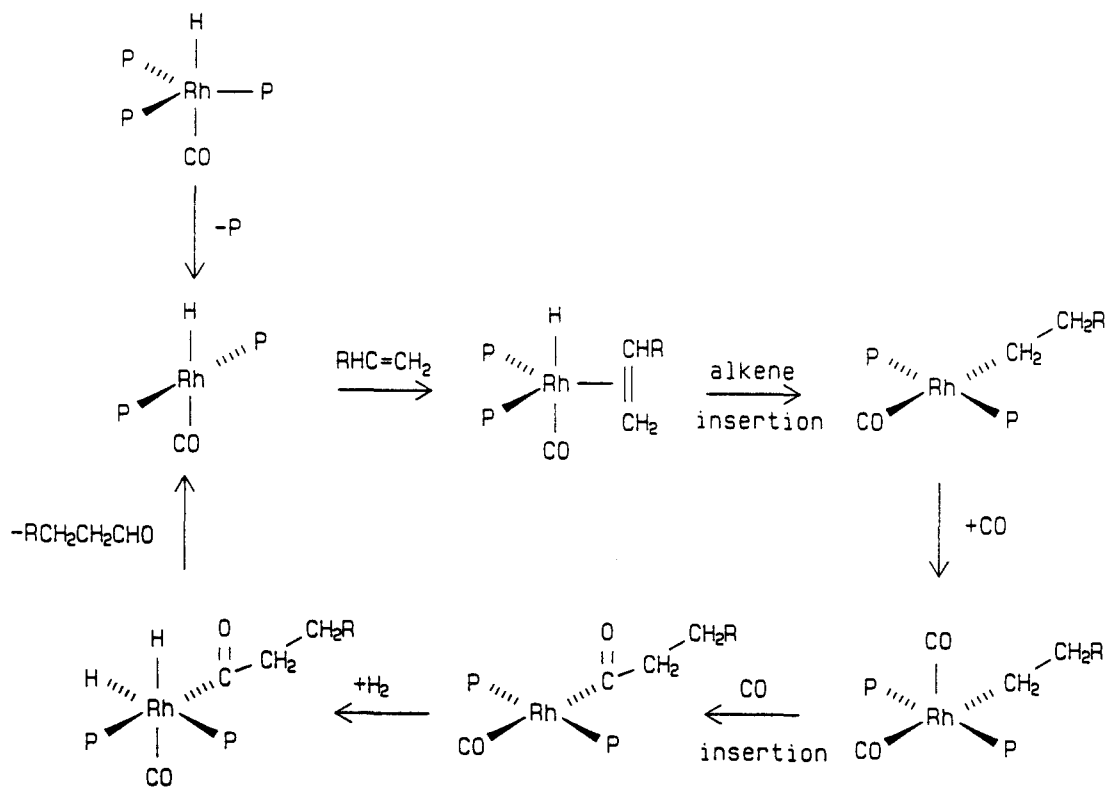
Heterogeneous catalysts are, at present, more widely used in industry than are homogeneous ones. There are several reasons for this preference. Heterogeneous catalysts are easily separated from the reactants and products of a process and, as well, these catalysts tend to be robust and readily recovered. The industrial preparation of ammonia by the Haber process is a typical example of the use of a heterogeneous catalyst. In this reaction, nitrogen reacts with hydrogen over an iron catalyst at pressures of 10^3 atmospheres and temperatures of approximately 500°C .⁹



The major disadvantage in using these catalysts is their lack of selectivity. That is, there are often several products formed, of which only one is desired. Furthermore, most heterogeneous catalysts require a combination of high reaction temperatures and pressures. Clearly, one cannot make thermally unstable compounds under such conditions.

It is for these reasons that homogeneous catalysts have been developed. Such complexes can usually operate under much milder conditions than heterogeneous catalysts and can be tailor-made to yield one predominant product. For example, *trans*-[Rh(CO)H(PPh₃)₃] is a catalyst used to hydrogenate olefins. It was found that, this complex specifically hydrogenates alk-1-enes in preference to alk-2-enes. On addition of carbon monoxide to the system, straight chain aldehydes are produced, as opposed to branched chain products.¹⁰ This rhodium complex operates efficiently at much lower temperatures and pressures than most heterogeneous catalysts. (see Scheme 1)

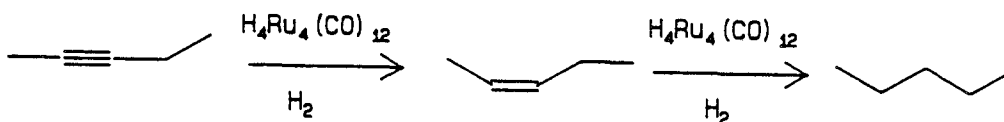
The major disadvantage in using homogeneous catalysts, however, is the difficulty in separating the catalyst from the products formed. Moreover, homogeneous catalysts are, in general, more fragile than their heterogeneous counterparts, making them less practical for industrial use.



Scheme 1 : Hydroformylation of an alkene to produce a straight chain aldehyde, catalyzed by $\text{trans-}[\text{RhH}(\text{CO})(\text{PPh}_3)_3]$.

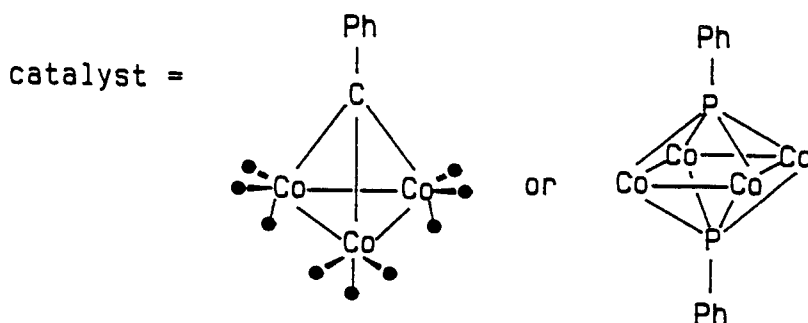
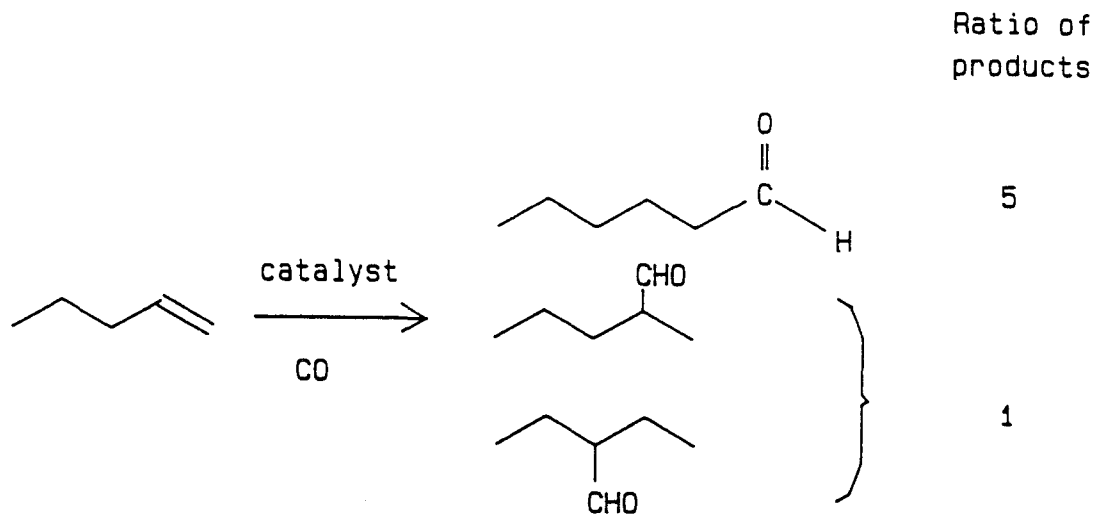
Transition metal clusters can be viewed as a compromise between homogeneous and heterogeneous catalysts. They can act as a controllable microsurface of three or four metal atoms, yet can be fashioned to suit a particular catalytic process, thereby rendering them highly specific.

Some clusters are already in use as catalytic species. For example, hydrogenation of C-C multiple bonds using hydrido carbonyl clusters is a well-established process.¹²



Further, there are cases in which cobalt clusters are used in hydroformylation reactions.¹³ Examples of these include PhCCo₃(CO)₉ and (PhP)₂Co₄(CO)₁₀.

The most widely known cobalt species used in the hydroformylation process is dicobalt octacarbonyl, Co₂(CO)₈. However, this is not considered to be a "true cluster catalysis", as the active agent is believed to be HCo(CO)₄, and not the dimeric cobalt species.¹⁴



1.3 The Importance of Developing Chiral Clusters

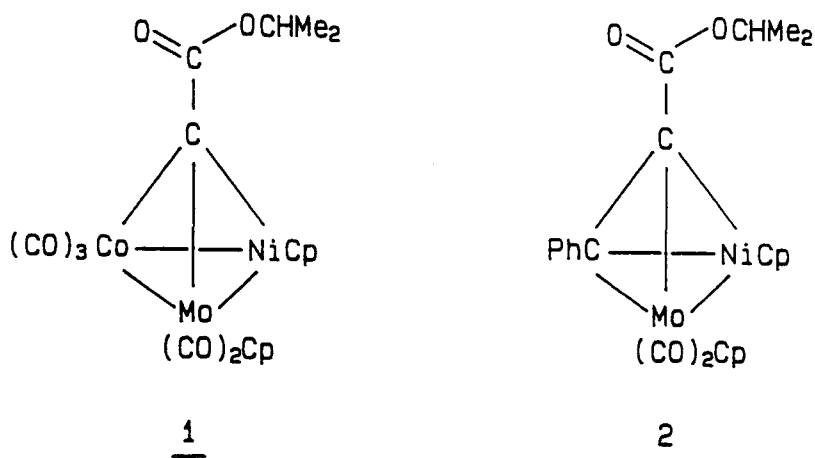
The development of processes which yield enantiomerically pure products is becoming increasingly important to the pharmaceutical industry. In most cases, if a molecule has two enantiomeric forms, only one of them has any medicinal use. An example of this is dihydroxyphenylamine, commonly referred to as DOPA. The L isomer is used in the treatment of Parkinson's disease, whereas D-DOPA would not have any beneficial effect to a Parkinson's patient.¹⁵ A more dramatic example of the importance of

producing one enantiomer over another, is the thalidomide problem that occurred in the 1960's.¹⁶ At that time, pregnant women were given a racemic mixture of this drug to help prevent morning sickness. It was later discovered that this medication caused their children to be born with severe birth defects. It has recently been shown that only one isomer of thalidomide, the S - isomer, is embryotoxic.¹⁶ If the women had been given an enantiomerically pure drug, this tragic problem would never have arisen. It is readily apparent that a general route to the preparation of enantiomerically pure species is very important.

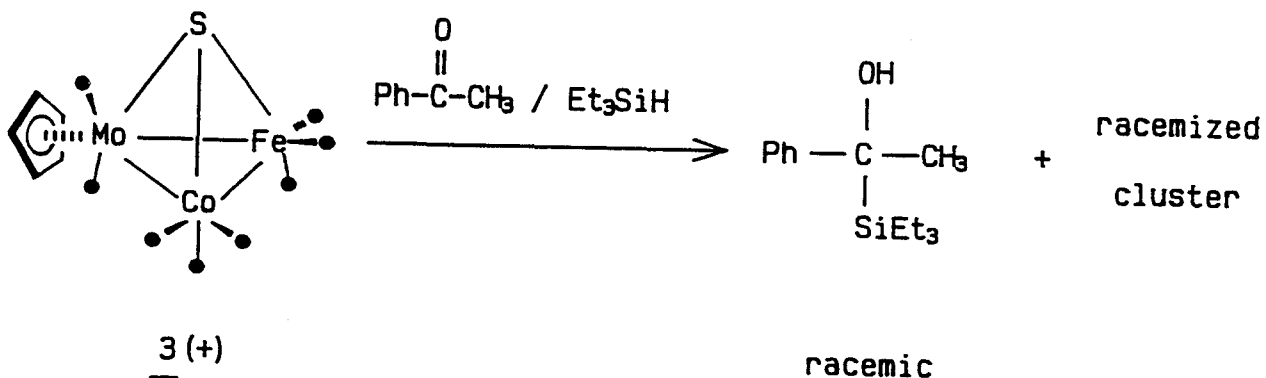
Assuming clusters will eventually play an important role in catalysis, it follows that chiral clusters could catalyze processes in which chiral products were obtained. Further, if the chiral cluster was enantiomerically pure, this should also be the case for the products from the catalytic process.

1.4 Routes to Developing Chiral Clusters

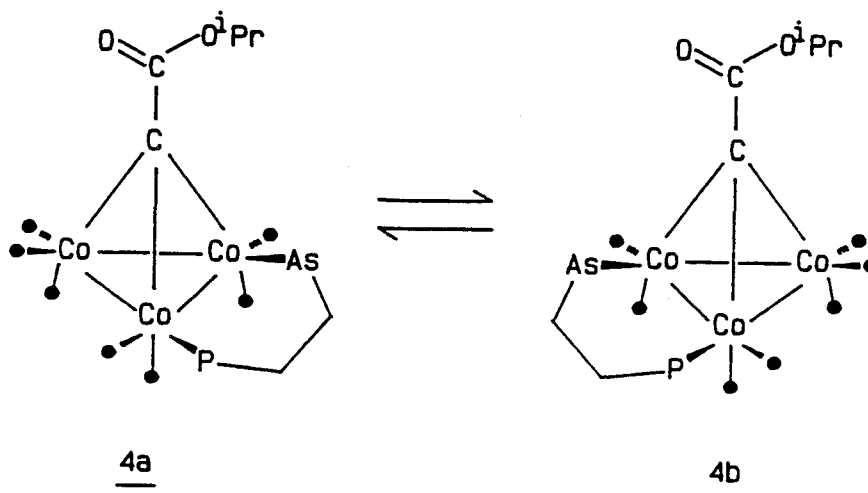
Early work in the development of chiral clusters involved constructing a tetrahedral cluster with four different vertices,^{17,18} such as 1 and 2.



The major problem with this method is enantiomer separation. However, even if this separation could be readily achieved, chiral catalysis using complexes of this type is not very likely. The reaction conditions needed for catalysis are also the conditions needed to racemize small mixed metal clusters. For example, Vahrenkamp attempted hydrosilylation of a ketone using a chiral mixed metal cluster¹⁹, 3. The product obtained was found to be racemic; furthermore, the cluster itself had lost its stereochemical integrity during the course of the reaction.

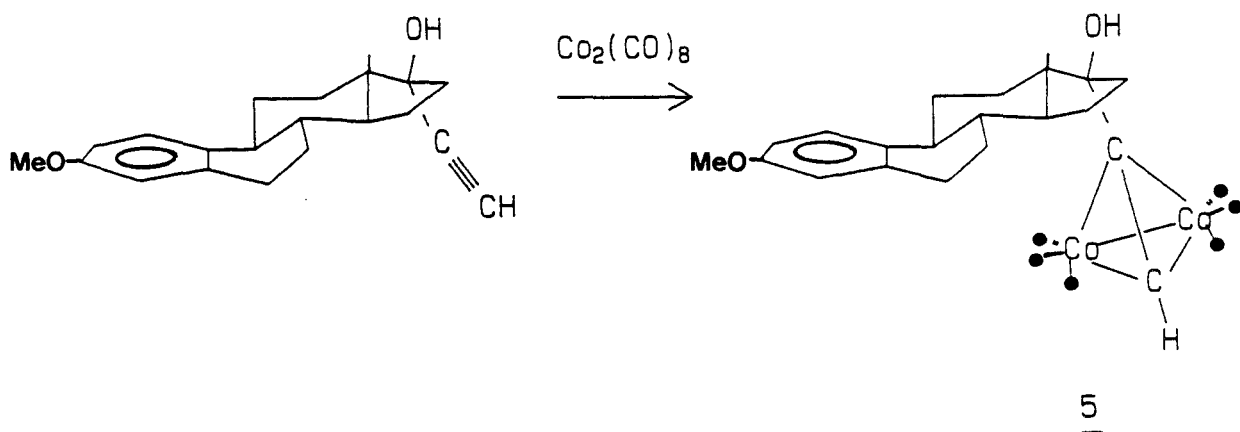


A much simpler approach to the synthesis of chiral clusters is incorporation of a non-symmetrical bidentate ligand into the cluster, as in 4.²⁰ This route is advantageous in that the production of the cluster can be done on a relatively large scale, as the arphos ligand, ie. $\text{Ph}_2\text{PCH}_2\text{CH}_2\text{AsPh}_2$, readily binds to the tricobalt species in quantitative yield. However, there is still the problem of enantiomer separation with which to contend. A more severe drawback in this system is caused by the fluxionality of these molecules;²⁰ the molecule racemizes on the NMR time scale via the migration of the arsenic terminus from one cobalt vertex to another.

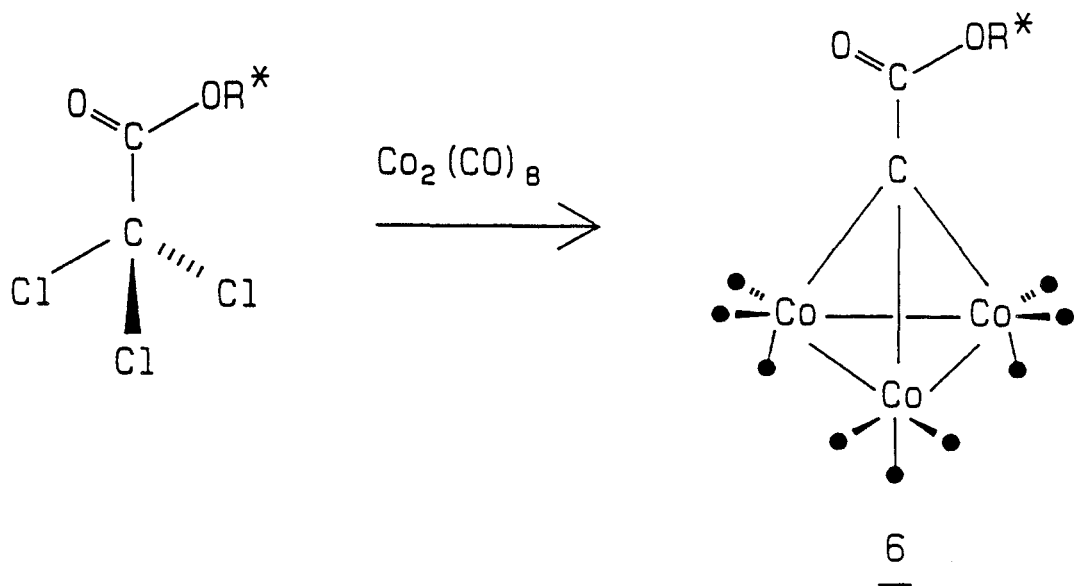


Finally, a third route to the production of chiral clusters is the incorporation of a chiral natural product into the molecule. There are two direct approaches

available. One possibility is the reaction between a steroidal alkyne and $\text{Co}_2(\text{CO})_8$. This yields a chiral dicobalt cluster of known absolute configuration.²¹ An example of this involves the reaction of mestranol with dicobalt octacarbonyl to give the cluster, 5.



A second possibility involves the reaction of $\text{Co}_2(\text{CO})_8$ with R^*CCl_3 , where R^* is derived from an enantiomerically pure natural product.^{22,23}



This approach yields enantiomerically pure, chiral clusters. There are numerous advantages in this method of cluster preparation and it is this route which we have chosen to follow.

1.5 Statement of Problem

In order to facilitate the relatively large scale production of enantiomerically pure clusters, several criteria need to be satisfied. Firstly, one must devise a straightforward method of attaching a trichloromethyl moiety to the natural product; secondly, after formation of the corresponding tricobalt nonacarbonyl cluster, there must be a simple means of replacing one of the $\text{Co}(\text{CO})_3$ vertices by an isolobal group such as the $(\text{C}_5\text{H}_5)\text{Mo}(\text{CO})_2$ or the $(\text{C}_5\text{H}_5)\text{Ni}$ fragment. Finally, it is necessary to incorporate convenient probes to allow the detection of the ratio of diastereomers from any given reaction.

CHAPTER TWO : PROBES FOR CHIRALITY

2.1 Concepts of Chirality

Before embarking on a detailed discussion of the synthetic and spectroscopic data on the series of molecules that has been examined in this project, one could profitably consider the concept of chirality as applied to these mixed metal systems. Looking at a relatively simple system, a substituted ethane molecule, one can see that this structure possesses C_1 symmetry. That is, every point on the surface of this molecule is different from every other point.

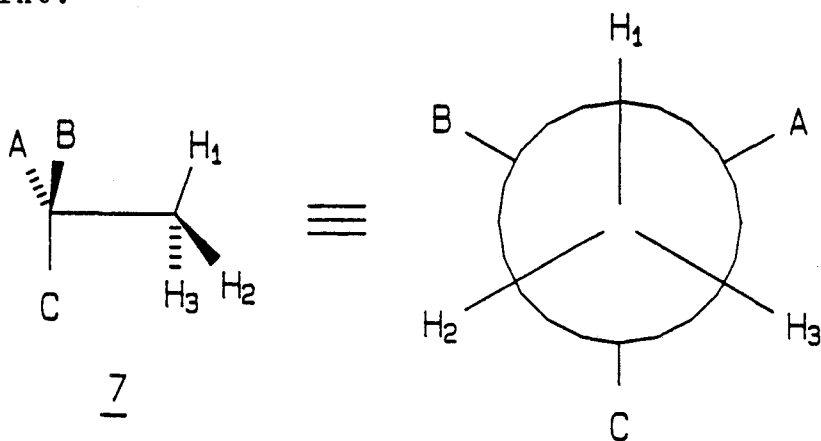


Figure 1 : A chiral substituted ethane molecule and its Newman projection.

However, a simple rotation of the methyl group interconverts all three protons. For example, considering the Newman projection in Figure 1, a 120° clockwise rotation puts H_1 in the position of H_2 , H_2 in the position of H_3 , etc. Therefore, one would observe a single methyl peak in the 1H NMR of this molecule because all three proton environments are being equilibrated. Substitution of H_3 by another group, X, will render H_1 and H_2 diastereotopic. In this case, a 120° rotation of the methyl group will not interconvert the protons. Examination of Figure 2 will show that the environments of H_1 and H_2 have *not* been equilibrated.

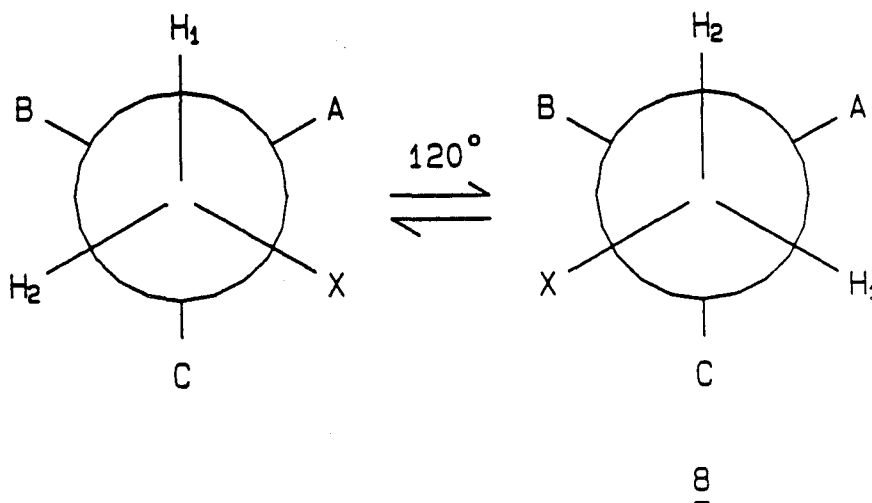


Figure 2 : A chiral substituted ethane molecule depicting diastereotopic protons, H_1 and H_2 .

Therefore, the proton NMR of this molecule will show two signals, one for each diastereotopic proton nucleus. Furthermore, each peak will be a doublet because of mutual coupling.

In order to interconvert the resonance frequencies of diastereotopic nuclei, it is necessary to bring about racemization of the system. Thus, if the asymmetric centre in the ethane, 8, can lose its stereochemical integrity via some appropriate mechanism, the methylene proton environments will be equilibrated. Such a process is exemplified in Figure 3.

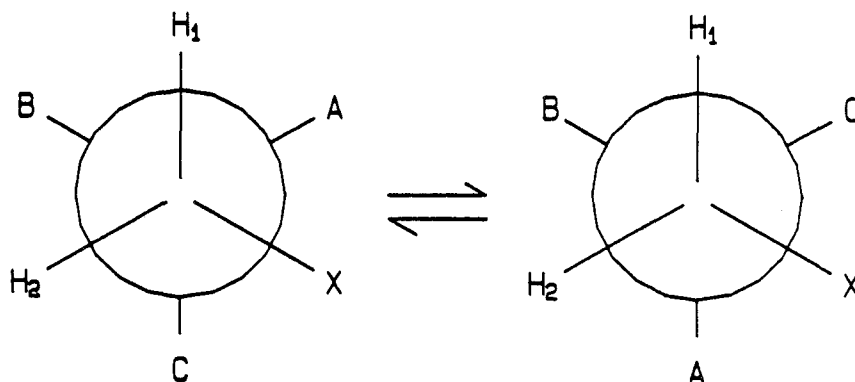


Figure 3 : Equilibration of the methylene proton environments via racemization of the system.

These concepts can be applied to analogous metallic systems. If one substituted the methyl protons in Figure 2

with cobalt nuclei, the same conclusions could be drawn, viz., the three cobalt atoms can be equilibrated by a simple rotation. Two of the cobalts can be made diastereotopic by substitution of the third cobalt by another metal such as molybdenum. This system is analogous to a mixed metal cluster with a chiral capping group, as in 10. (see Figure 4)

The cobalt vertices can also be rendered diastereotopic by incorporation of a bidentate ligand into the molecule. The bidentate ligand need not be unsymmetrical; it is sufficient that the cobalt nuclei in this cluster cannot be interconverted by simple rotation of a molecular segment. One should note that the ligands (e.g., phosphines) attached to the diastereotopic cobalts are likewise magnetically non-equivalent.

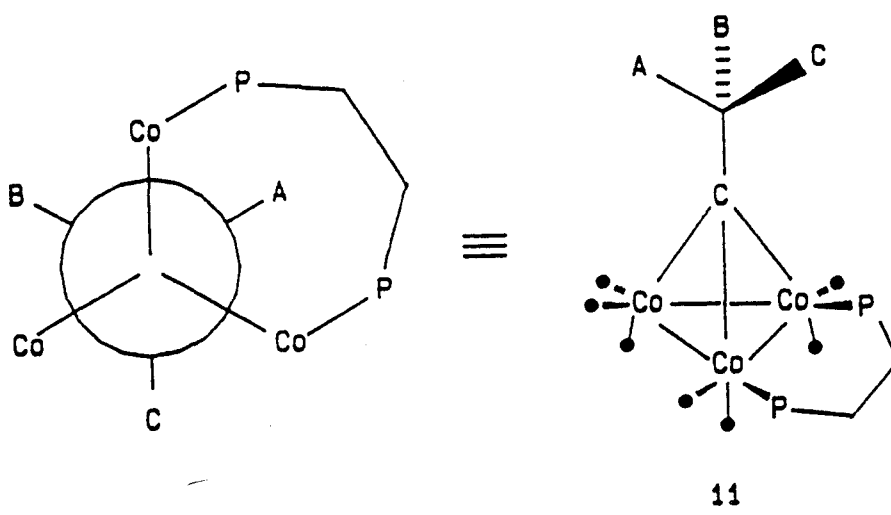


Figure 5 : Incorporation of a bidentate ligand into a chiral tricobalt cluster renders the cobalt vertices diastereotopic.

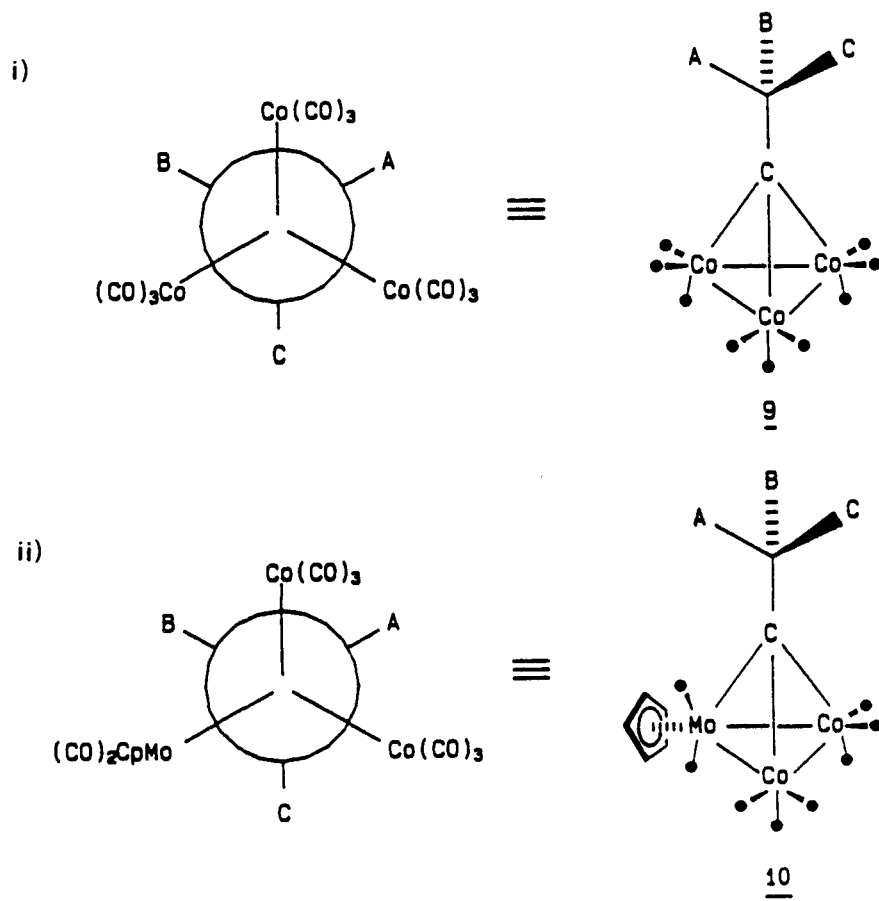


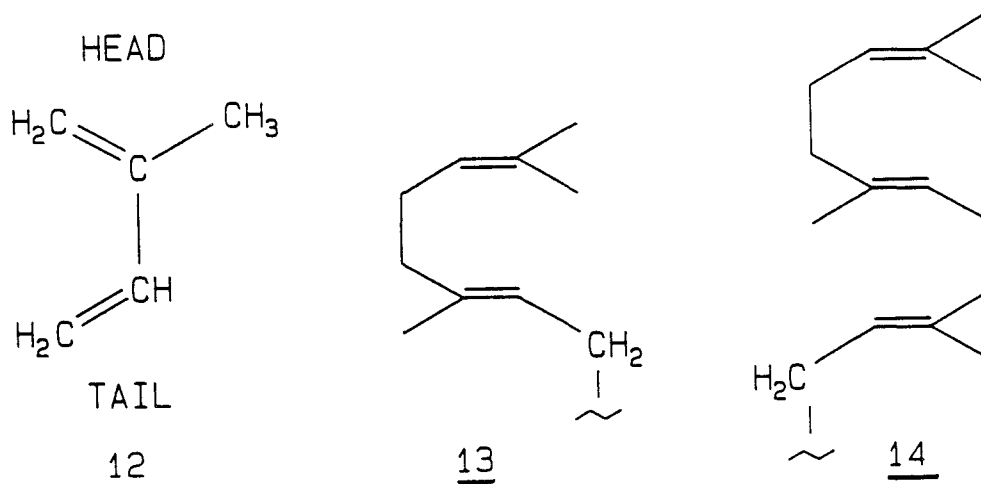
Figure 4 : Analogous transition metal systems.

i) a chiral tricobalt cluster

ii) a chiral mixed metal cluster in which the two cobalt nuclei are diastereotopic.

2.2 Chiral Substituents

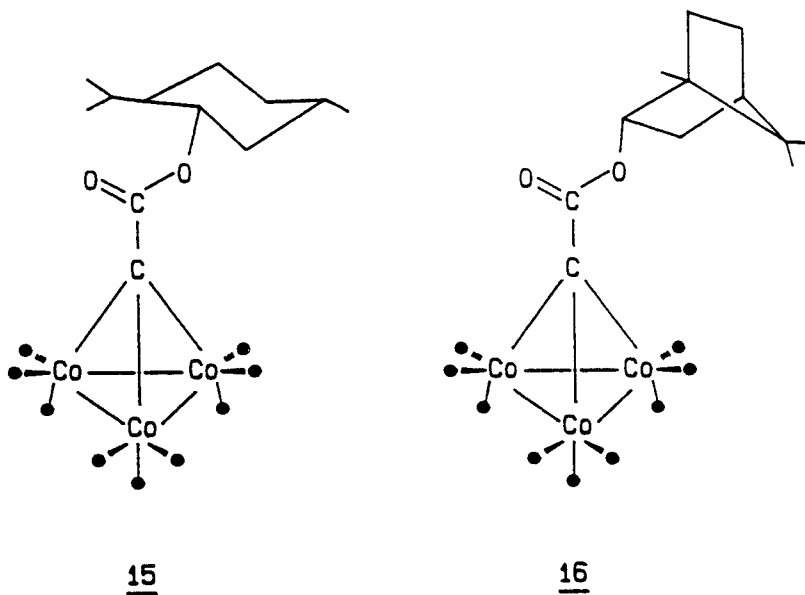
Incorporation of a chiral natural product into a cluster will render the cluster itself chiral. We chose to use terpenes as our source of chirality. Terpenes are natural products that are found in most plants. They are derived ultimately from isoprene, 12, which can be coupled to give geranyl, 13, or farnesyl, 14, derivatives. These in turn can yield squalene which is a precursor of the steroidal skeleton.²⁴



Monoterpenes are those terpenes which contain two isoprene units. Those which contain three isoprene units are called sesquiterpenes and those containing four, six, and eight units are called diterpenes, triterpenes and tetraterpenes, respectively. Such terpenes are formed when the isoprene units combine in a head to tail manner. These natural

products are readily available, inexpensive and can be obtained as enantiomerically pure species. In some cases, both enantiomers are commercially available. This latter point is important since one might develop an efficient catalytic system which yields an enantiomerically pure product but of the opposite chirality to that which was required. In that case, it would merely be necessary to start from the other enantiomer of the terpene. Two monoterpenes have been employed in this study, viz., (1R, 3R, 4S)(-)-menthol and (1R-*exo*)(+)-borneol. Before these molecules could be built into a cluster, it was necessary to convert them into a more suitable form, namely an α,α,α -trichloro species. The menthol and exoborneol were each treated with trichloroacetylchloride to produce their respective trichloroacetate esters. These esters then reacted with dicobalt octacarbonyl to produce the corresponding clusters, 15 and 16.^{8,23}

The synthesis of these clusters was relatively straightforward and could be achieved in good yield. It was now our goal to incorporate a probe into the molecule to detect this chirality.



2.3 NMR Probes for Chirality

The concept of building an NMR probe into a cluster is not a novel one. Previous work has been done with the chiral complex, $\text{Co}_3(\text{CO})_7(\text{arphos})\text{CCO}_2\text{CHMe}_2$, 4.²⁰ In this molecule the arsenic terminus migrates from one cobalt vertex to another, racemizing the cluster on the NMR time scale. This fluxionality was monitored by ^{13}C and proton NMR using the apical isopropyl group as a probe. Figure 6 depicts the variable temperature proton spectra of 4. At room temperature, the diastereotopic methyl groups are equilibrated giving a single resonance in the ^1H NMR spectrum. (Actually, the resonance appears as a doublet because the methyls couple to the contiguous CH of the

isopropyl group). However, on cooling the sample, the interconversion of enantiomers is slow, and each methyl group gives rise to a separate doublet signal.

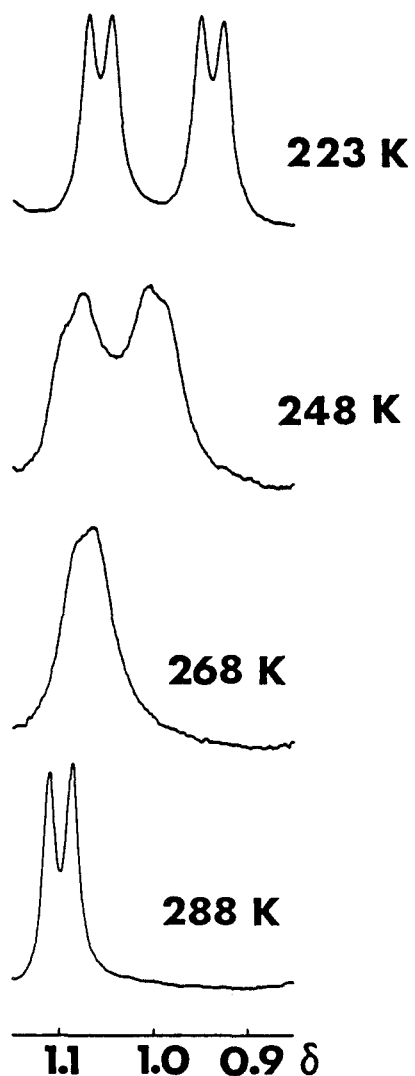
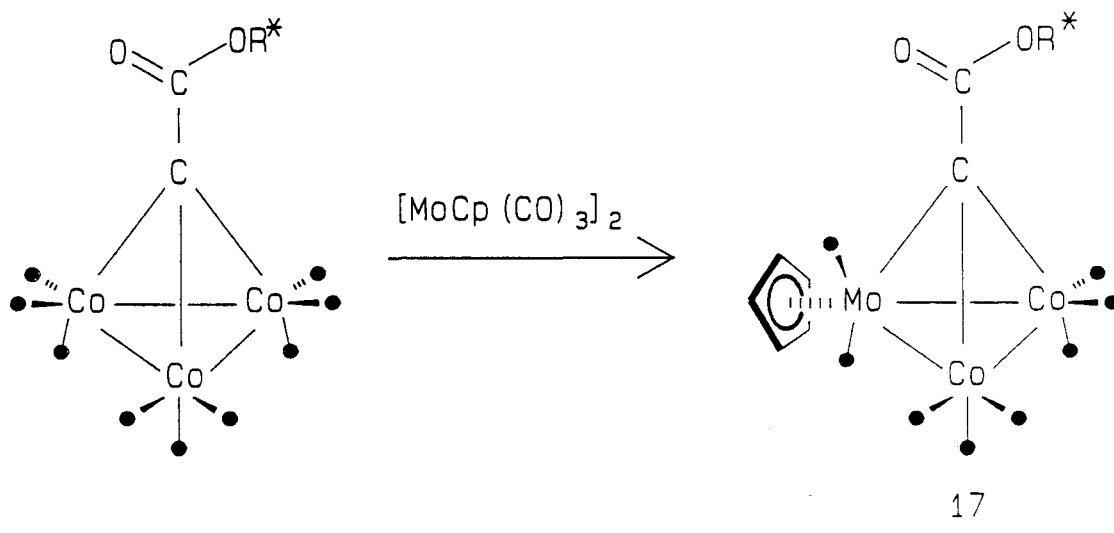


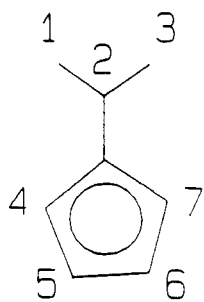
Figure 6 : Variable temperature 250 MHz ^1H NMR spectra of the methyl region of $\text{Co}_3(\text{CO})_7(\text{arphos})\text{CCO}_2\text{CHMe}_2, 4$.

In the $\text{Co}_3(\text{CO})_9\text{CCO}_2$ -menthyl molecule, it is not possible to incorporate a probe into the apical group of the cluster, as the source of chirality viz., the terpene is already occupying this position. In this complex, a probe must be built into one of the metal vertices.

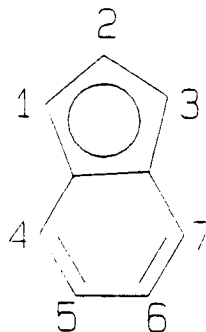
A very well known reaction that tricobalt clusters undergo is the replacement of one of the $\text{Co}(\text{CO})_3$ units by an isolobal $\text{Mo}(\text{CO})_2\text{Cp}$ fragment.^{25,26} This is accomplished by refluxing the tricobalt cluster with an excess of the molybdenum dimer under a nitrogen atmosphere.



It was our intent to include a probe for chirality within the cyclopentadienyl ring of the molybdenum dimer. There were two probes which we wished to employ. The first was the isopropylcyclopentadienyl ligand, $\text{C}_5\text{H}_5\text{CHMe}_2$, 18; the second was the indenyl system, 19.



18



19

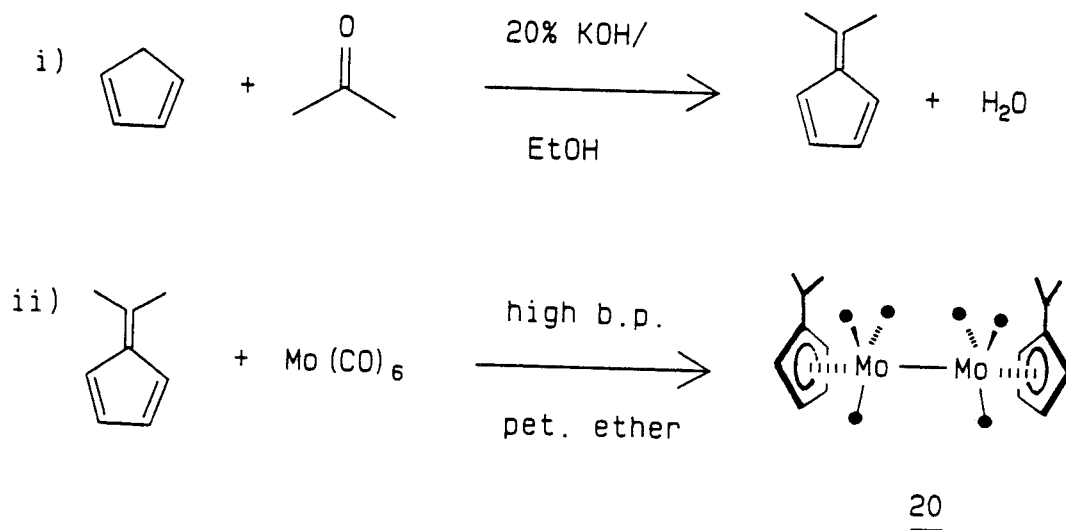
Both of these molecules have C_{2v} symmetry. That is, they possess two mirror planes and a C_2 axis. Coordination on one face to a metal still maintains one mirror plane and the local symmetry is now C_s . Therefore, C(1) is equivalent to C(3), C(4) is equivalent to C(7) etc. However, if these ligands are incorporated into a chiral molecule, this would render all the carbons inequivalent. That is, C(1) and C(3) should now give different signals in the NMR spectrum as they are in environments which are magnetically different.

2.4 Synthesis and Characterization of the Molybdenum

Dimers

Incorporation of these probes into molybdenum dimers was our next concern. This was readily accomplished using known literature preparations. The first step in

this procedure involved the preparation of 6,6-dimethylfulvene from the reaction of acetone and the anion derived from cyclopentadiene.²⁷



The dimethylfulvene was then heated at reflux with $\text{Mo}(\text{CO})_6$ in high boiling petroleum ether²⁸, yielding a fine red crystalline solid, $[\text{Mo}(\text{C}_5\text{H}_4\text{-CHMe}_2)(\text{CO})_3]_2$, 20.

Similarly, the indenyl molybdenum dimer was prepared by heating indene and $\text{Mo}(\text{CO})_6$ at reflux in high boiling petroleum ether.²⁹ A fine, brown, air-sensitive powder, 21, was produced in very low yield (13%).

Both products were identified using Fast Atom Bombardment (FAB) mass spectrometry, infra-red and carbon-13 NMR spectroscopy. The FAB mass spectrum of 20 is shown in Figure 7. Molybdenum has seven natural isotopes which accounts for the complex isotopic pattern.

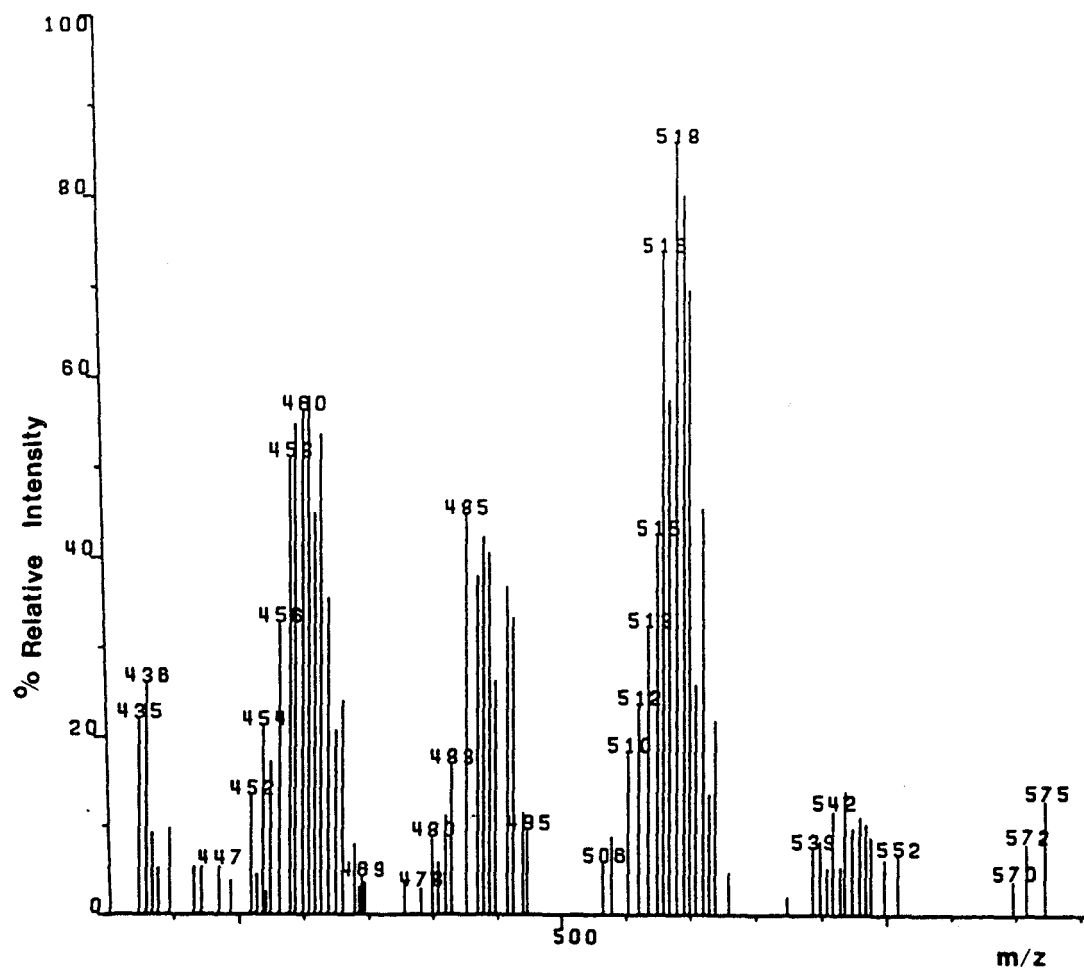


Figure 7 : High mass region of the FAB mass spectrum of $[(C_5H_4-CHMe_2)Mo(CO)_3]_2$, 20.

2.5 Results

The carbon-13 NMR spectrum of $[\text{Mo}(\text{C}_5\text{H}_4\text{-CHMe}_2)(\text{CO})_3]_2$, 20, showed one signal in the methyl region, attributed to carbons 1 and 3. On incorporation of the molybdenum isopropyl cyclopentadienyl moiety into the cluster, 15, the mixed metal system, $\text{Co}_2(\text{CO})_6\text{Mo}(\text{C}_5\text{H}_4\text{-CHMe}_2)(\text{CO})_2\text{C-CO}_2\text{menthyl}$, 22, was obtained. The carbon-13 NMR spectrum of 22 exhibits five methyl resonances. These are assignable to three methyl groups of the menthyl substituent and the two diastereotopic methyl groups of the isopropyl fragment on the cyclopentadienyl ring.

Similarly, C-13 NMR spectra were measured for both the molybdenum indenyl dimer, 21, and the mixed metal cluster, 23. The C(1) and C(3) positions in the five-membered ring are the most useful to observe, since they are the closest to the metal and also bear protons, which, by virtue of their nuclear Overhauser effect, enhance the sensitivity of the C-13 signals.

The carbons at positions 1 and 3 of the dimer give one signal at 84.1 ppm. There is also a peak at 93.4 ppm accounted for by the C(2) carbon on the five-membered ring (see Figure 8). The cluster, 23, shows a resonance at 92.8 ppm for C(2), but shows two other resonances at 84.0 and 82.1 ppm for carbons 1 and 3, which are now diastereotopic.

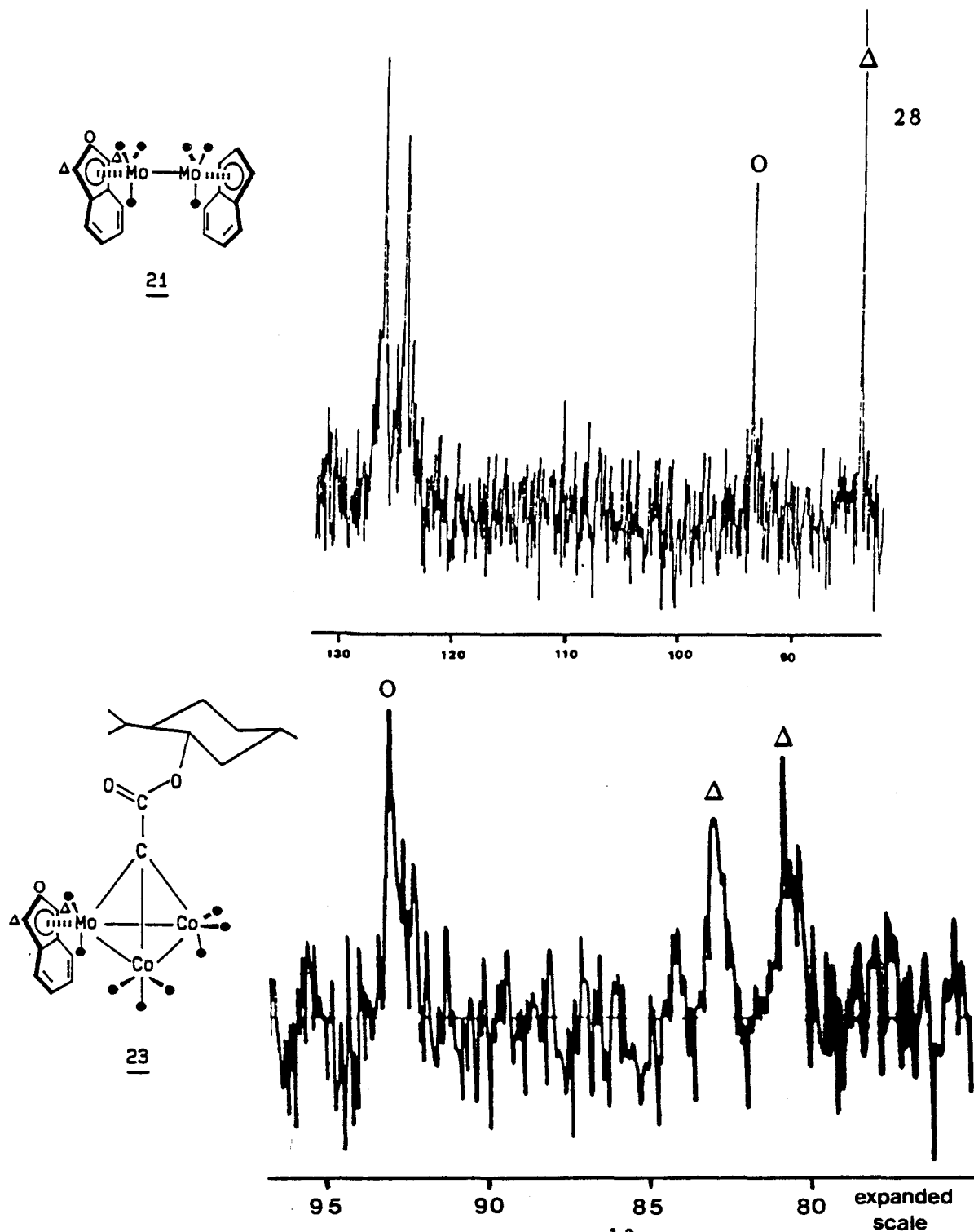


Figure 8 : a) Section of the 62.8 MHz ^{13}C spectrum of $[(\text{C}_9\text{H}_7)\text{Mo}(\text{CO})_3]_2$, 21.
 b) Section of the 125.7 MHz ^{13}C spectrum of $\text{Co}_2(\text{CO})_6\text{Mo}(\text{CO})_2(\text{C}_9\text{H}_7)\text{CCO}_2\text{menthyl}$, 23, showing the splitting of the indenyl five-membered ring carbons, C(1) and C(3).

Both the isopropyl-cyclopentadienyl and the indenyl ligands have proven to be effective probes for chirality. However, the indenyl ligand offers one major advantage. That is, the C-13 signals of interest are downfield in the 80-90 ppm region, whereas, the methyl signals in the $C_5H_4-CHMe_2$ unit come up amidst a sea of methyl peaks, making them much more difficult to assign.

2.6 Further Study with the Indenyl Probe

In the cluster 23, the mirror symmetry of the indenyl ligand has been broken because of the presence of the chiral capping group. This caused a doubling of the previously equivalent C(1) and C(3) nuclei within the same molecule. Incorporation of an arphos ligand into this cluster brings about a further splitting of these peaks. The C(2) resonance is also split. This comes about because the arphos can bind in two ways, as in 24 and 25, thus yielding a diastereotopic mixture in the ratio 54/46 as indicated by the C-13 NMR spectrum shown in Figure 9.

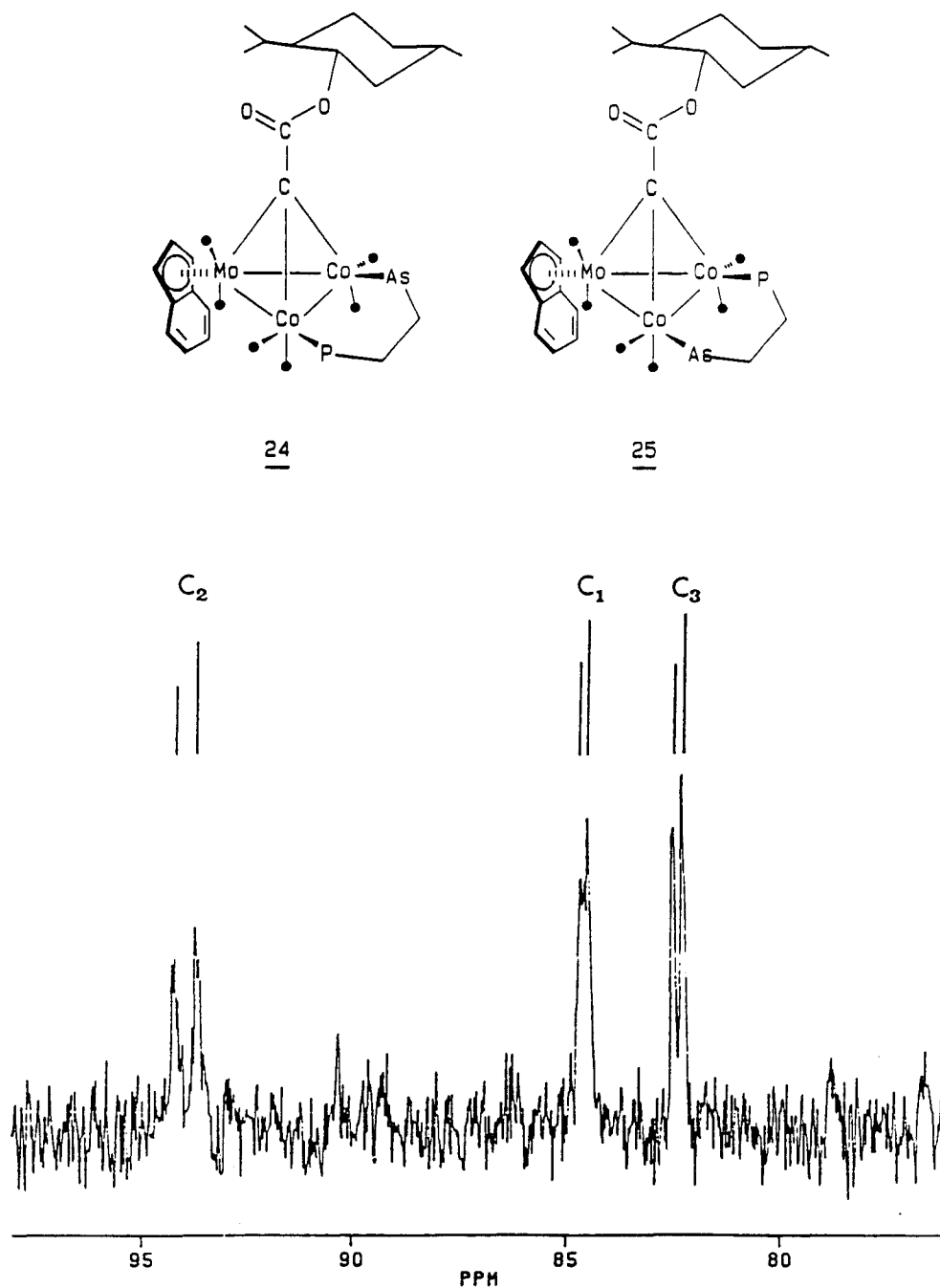
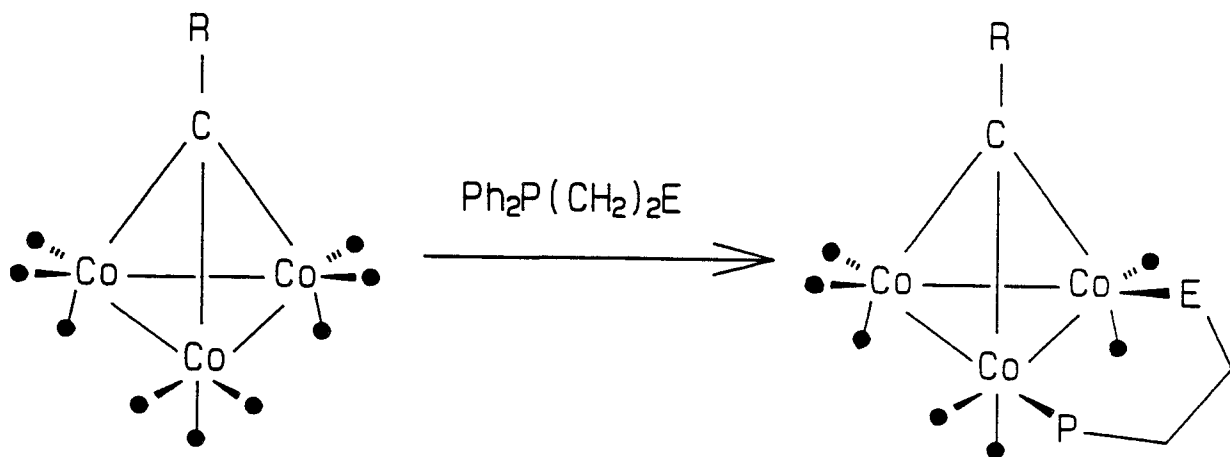


Figure 9 : Section of the 125.7 MHz ¹³C NMR spectrum of the diastereomers of Co₂(CO)₄(arphos)-Mo(CO)₂(C₉H₇)CCO₂menthyl, 24 and 25, showing the further splitting of the indenyl five-membered ring carbons, C(1), C(2) and C(3).

CHAPTER THREE : REACTIONS OF CHIRAL CLUSTERS
WITH BIDENTATE LIGANDS

3.1 Incorporation of the Diphos Ligand

Treatment of alkylidyne clusters of the type $RCo_3(CO)_9$ with a bidentate ligand, e.g., $Ph_2PCH_2CH_2PPh_2$ (diphos), leads to the replacement of two carbonyls and the formation of a chelate ring, as in 26.



26 E=PPh₂

27 E=AsPh₂

If the cluster being treated is achiral, then the two phosphorus atoms in the chelating ligand are equivalent. Therefore, one would expect to see only one signal in the P-31 NMR spectrum. This is indeed the case when $R=Cl$ ³⁰ or $R=CO_2CHMe_2$.²⁰ That is, the ³¹P NMR spectrum for the cluster $Co_3(CO)_7(diphos)CCO_2CHMe_2$ in C_6D_6 exhibits one peak at 42.0 ppm.²⁰ Similarly, $Co_3(CO)_7(diphos)CCl$ shows a single peak at 45.2 ppm in the phosphorus NMR.³⁰

However, when $R = CO_2menthyl$, the $Co(CO)_2P$ vertices are now diastereotopic and should thus exhibit two resonances in the P-31 NMR spectrum. One does indeed observe two phosphorus environments in the NMR, at all temperatures (see Figure 10). The spectrum at room temperature shows two rather broad peaks. These signals sharpen considerably as the sample is cooled. This broadness is not attributed to a chemical exchange process. Rather, it is caused by quadrupolar effects because of the proximity of the ⁵⁹Co nuclei ($I = 7/2$) to the phosphorus nuclei. The diphos ligand proves to be a convenient and effective probe for chirality.

3.2 Incorporation of the Arphos Ligand

Similarly, tricobalt clusters, $Co_3(CO)_9CR$, can be treated with an unsymmetrical bidentate ligand such as arphos, $Ph_2AsCH_2CH_2PPh_2$, to give 27.

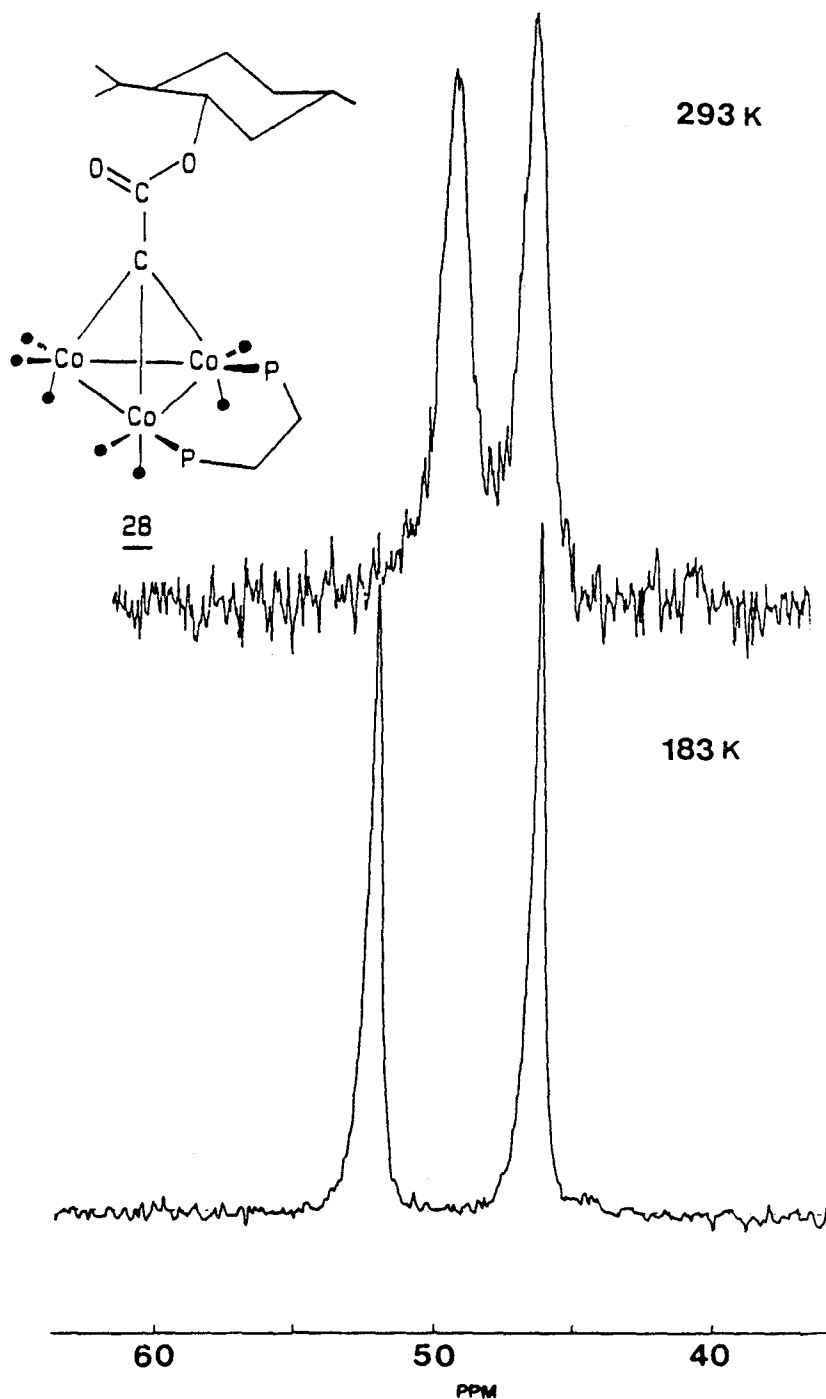
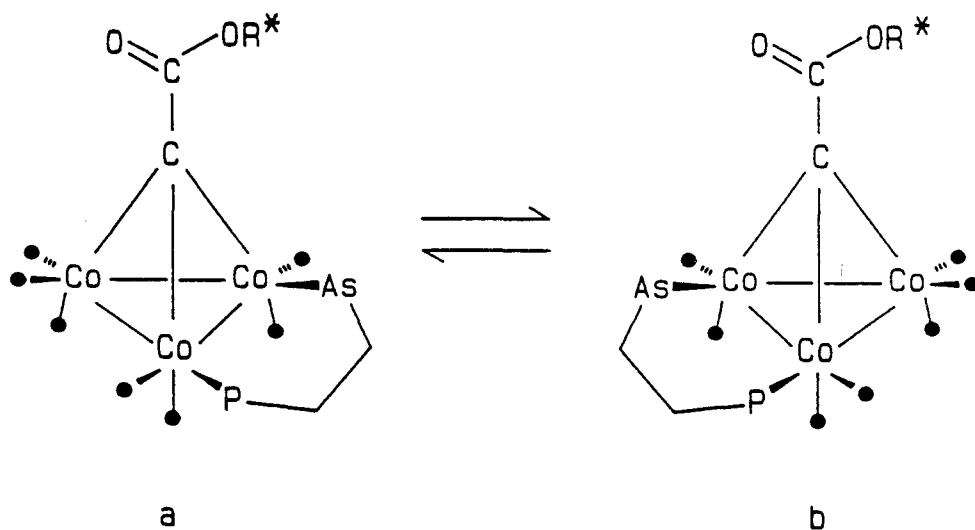


Figure 10 : 101.2 MHz variable temperature ^{31}P NMR spectra of $\text{Co}_3(\text{CO})_7(\text{diphos})\text{CCO}_2\text{menthyl}$, **28**, showing the clear differentiation of the diastereotopic phosphorus nuclei.

As previously discussed, arphos clusters are fluxional because the AsPh_2 terminus can migrate from one cobalt atom to another.²⁰ In the case of $\text{Co}_3(\text{CO})_7(\text{arphos})-\text{CCO}_2\text{CHMe}_2$, only one phosphorus signal is observed in the ^{31}P NMR spectrum at all temperatures. This is to be expected because the fluxional process is merely inter-converting enantiomers on the NMR time scale. The isopropyl capping group can be used to detect this racemization, as the two methyl groups are potentially diastereotopic. Both the variable temperature carbon-13 and proton spectra were used to evaluate ΔG^\ddagger for this process. The activation energy barrier for the inter-conversion of enantiomers was calculated as 13.1 ± 0.5 kcal/mole.²⁰



29 $\text{R}^* = \text{menthyl}$

30 $\text{R}^* = \text{exo-boronyl}$

If the apical group, R, however, were to be a chiral substituent, one could monitor the fluxionality of the molecule by P-31 NMR spectroscopy. In this case, the process no longer involves the racemization of a pair of enantiomers; it is an interconversion of diastereomers. That is, the phosphorus nucleus in 29a is not magnetically equivalent to the phosphorus nucleus in 29b (similarly with 30a / 30b). At room temperature, the P-31 NMR spectrum of 29 exhibits a singlet, indicating a rapid interconversion of the diastereomers a and b at this temperature. Upon cooling to -50°C, two phosphorus resonances are observed, showing that the migration of the arsenic terminus is now occurring at a rate slower than the NMR time scale. The variable-temperature ³¹P spectra are shown in Figure 11 and exhibit a coalescence pattern. The peak separation in the limiting spectrum at 203 K is 410 Hz and this, in conjunction with a coalescence temperature of 288 K yields an approximate activation energy barrier of 13.1 ± 0.5 kcal/mole. This barrier is calculated using the following equation:

$$\frac{\Delta G^\ddagger}{R \cdot T_c} = \ln(2 \cdot R / \pi \cdot N \cdot h) + \ln(T_c / \Delta\nu)$$

where T_c is the coalescence temperature and $\Delta\nu$ is the peak separation in Hertz for the limiting spectrum.

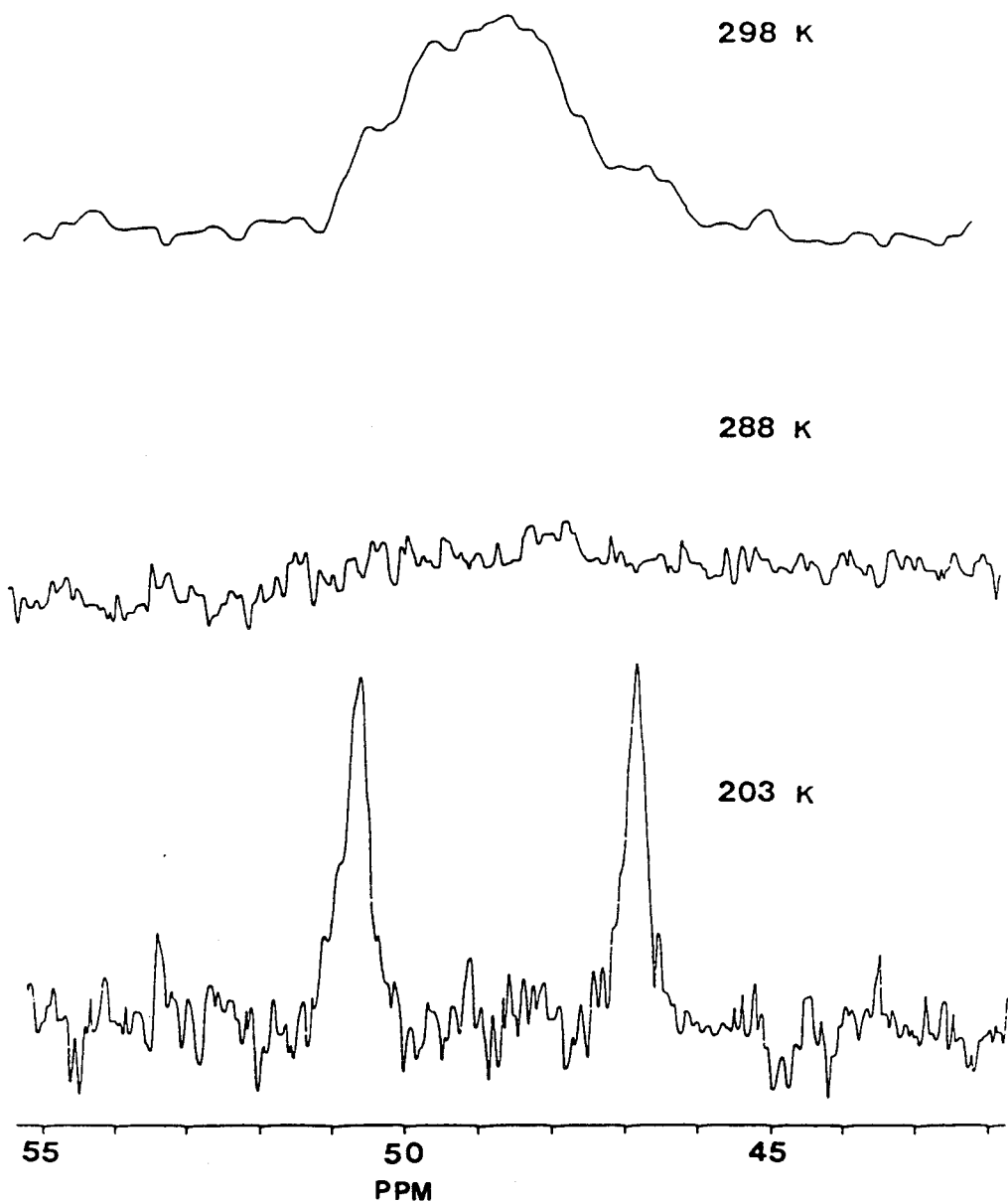


Figure 11 : 101.2 MHz variable temperature ^{31}P NMR spectra of $\text{Co}_3(\text{CO})_7(\text{arphos})\text{CCO}_2\text{menthyl}$, showing a slow interconversion of the diastereomers 29a and 29b at low temperature.

Similar results were obtained when R = *exo*-bornyl, 30. Again, variable-temperature P-31 NMR spectra were recorded and are shown in Figure 12. A coalescence temperature of approximately 270 K is observed and the peak separation in the limiting spectrum at 178 K is 178 Hz. However, in this molecule it is readily apparent that 30a and 30b are not present in equal amounts. There is a diastereomeric mixture in the ratio of $\approx 60 : 40$ as indicated by the P-31 NMR spectrum. This illustrates that one diastereomer is formed preferentially over the other, i.e., there is chiral discrimination occurring. The approximate activation energy calculated for this system was 12.6 ± 0.5 kcal/mole.

3.3 Computer Modelling of these Systems

The measured barriers for both systems studied, i.e., the menthyl system, 29, $\Delta G^\ddagger = 13.1 \pm 0.5$ kcal/mole and the *exo*-bornyl system, 30, $\Delta G^\ddagger = 12.6 \pm 0.5$ kcal/mole, compare favourably with the reported activation energy of 13.1 ± 0.5 kcal/mole for the racemization of $\text{Co}_3(\text{CO})_7\text{-(arphos)CCO}_2\text{CHMe}_2$, 4, which was monitored using the ^1H and ^{13}C NMR resonances of the isopropyl methyls. This implies that the large chiral apical group (menthyl or *exo*-bornyl) does not markedly hinder the migration of the arsenic terminus from one cobalt nucleus to another.

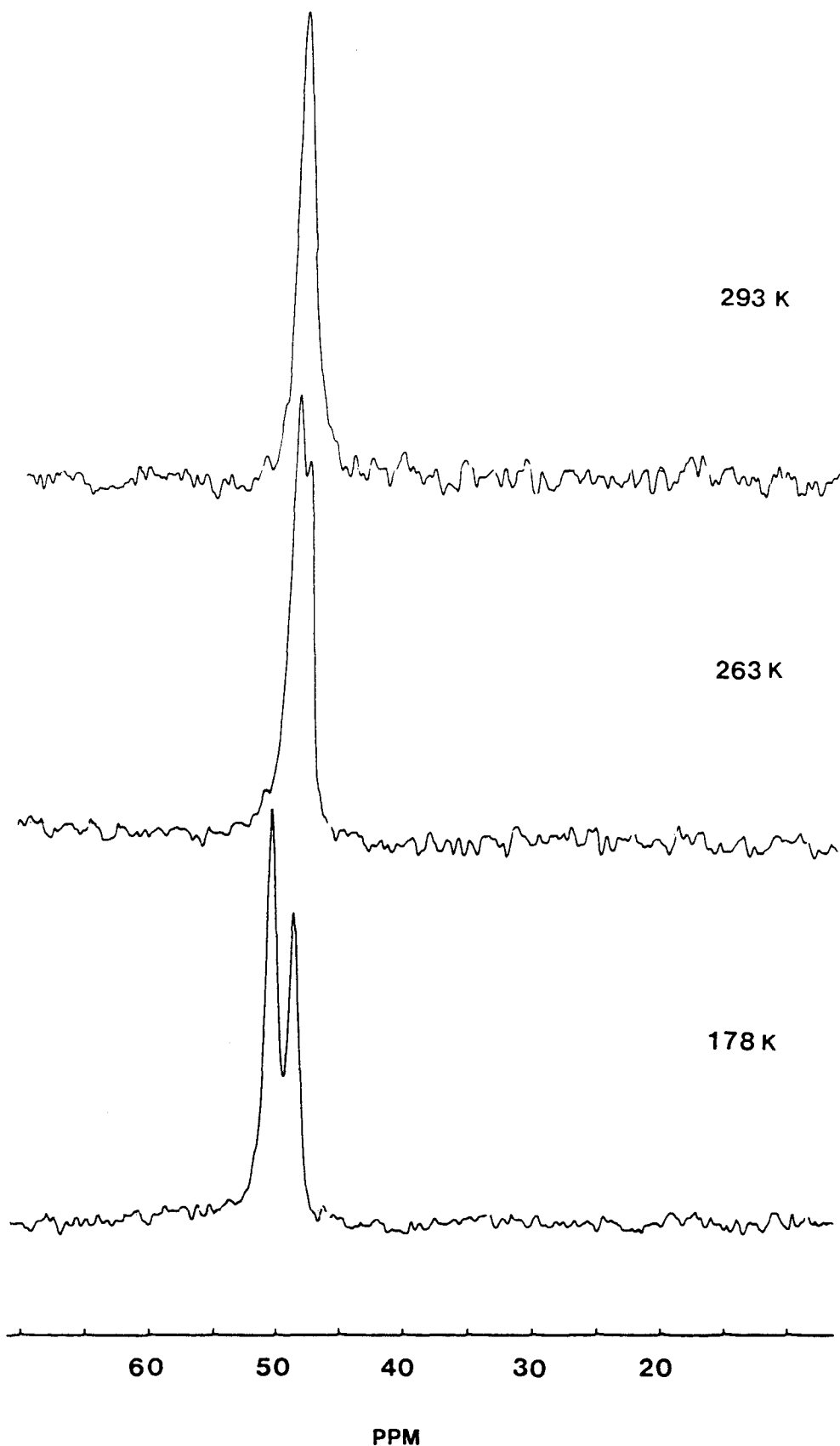


Figure 12 : 101.2 MHz variable temperature ^{31}P NMR spectra of $\text{Co}_3(\text{CO})_7(\text{arphos})\text{CCO}_2\text{-exo-bornyl}$, showing the slow interconversion of the diastereomers 30a and 30b at low temperature.

To determine if this was indeed the situation, the computer modelling system, Chem-X³¹ was employed. The crystal structure coordinates of a known tricobalt-arphos cluster²⁰ were used in conjunction with the coordinates of menthol³² to obtain a model of $\text{Co}_3(\text{CO})_7(\text{arphos})\text{CCO}_2\text{menthyl}$, 29. This model was compared to the structure of $\text{Co}_3(\text{CO})_7(\text{arphos})\text{CCO}_2\text{CHMe}_2$.²⁰

The Chem-X models of the two clusters show that neither capping group appears to pose any major steric hindrance to the arphos fluxionality (see Figures 13 and 14).

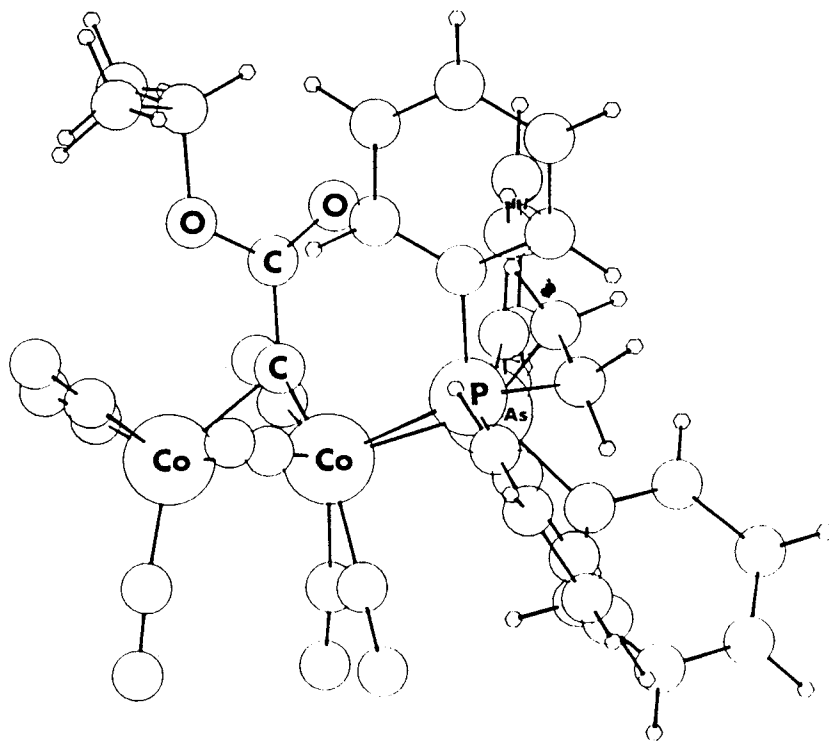


Figure 13 : Chem-X model of $\text{Co}_3(\text{CO})_7(\text{arphos})\text{CCO}_2\text{CHMe}_2$, 4.

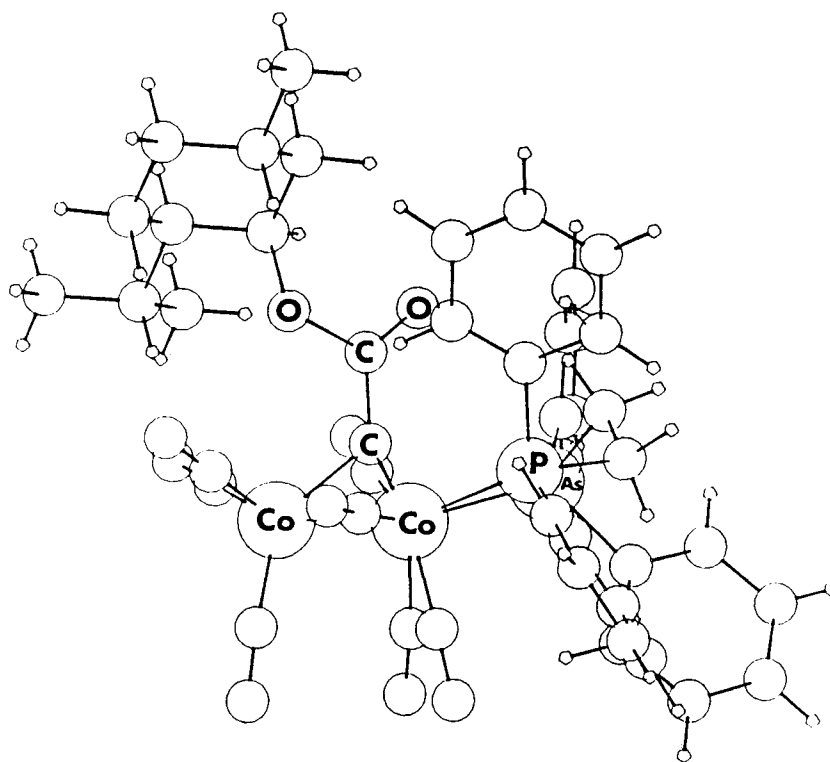
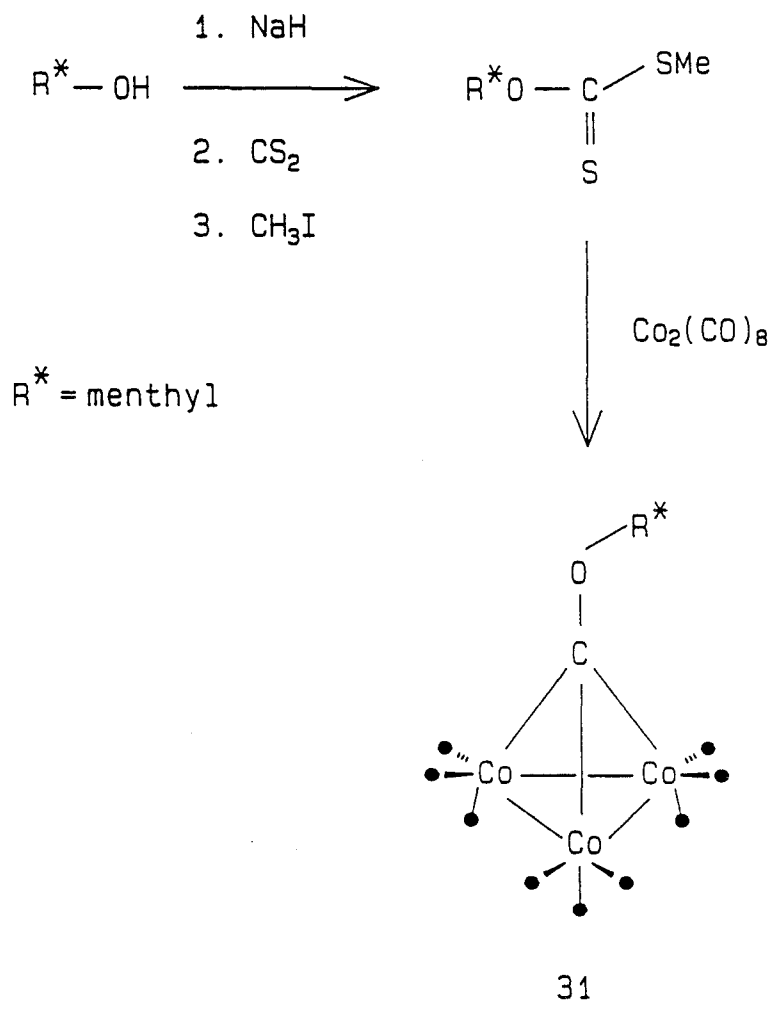


Figure 14 : Chem-X model of $\text{Co}_3(\text{CO})_7(\text{arphos})\text{CCO}_2\text{menthyl}$, 29.

3.4 Related Work in this Area

Other work in our laboratory³³ has involved bringing the chiral capping group closer to the cluster. This involved synthesizing a molecule in which the terpenoidal fragment was separated from the cluster by an ether group rather than an ester group^{33,34,35} (see Scheme 2).



Scheme 2 : Synthesis of $\text{Co}_3(\text{CO})_9\text{C-O-menthyl}$, 31.

Subsequent treatment of the cluster, 31, with arphos yielded $\text{Co}_3(\text{CO})_7(\text{arphos})\text{C-O-menthyl}$, 32, as expected. It was anticipated that the energy barrier for the migration of the $-\text{AsPh}_2$ moiety would be increased because of steric hindrance from the apical group. However, variable-temperature P-31 NMR spectra of this cluster were recorded and showed only one peak at 43.9 ppm at all temperatures. As can be seen from the Chem-X model of this molecule (Figure 15), the cluster is terribly hindered. It is possible that only one diastereomer is formed in this reaction, and that the fluxional arphos process is not occurring because of steric factors. It is obvious that further investigation of this system is necessary.

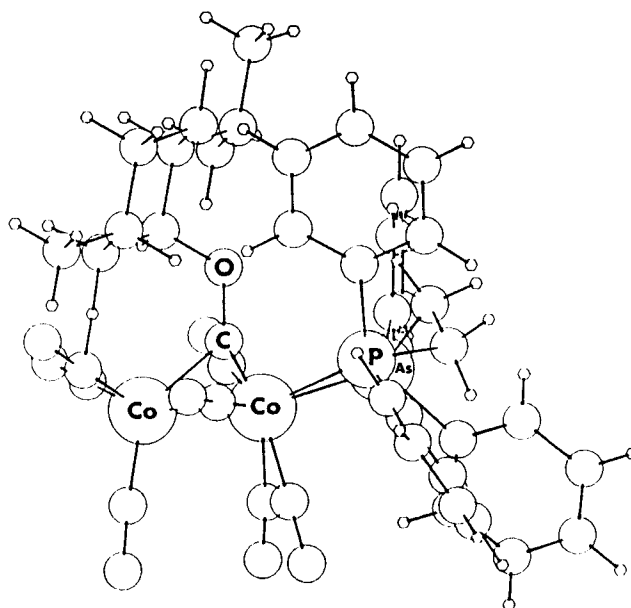


Figure 15 : Chem-X model of the tricobalt ether cluster, $\text{Co}_3(\text{CO})_7(\text{arphos})\text{C-O-menthyl}$, 32.

3.5 Characterization of the Chiral Clusters

The products synthesized were characterized using a number of techniques. These include melting point, thin layer chromatography, FAB mass spectrometry, elemental analysis, IR and NMR spectroscopy.

The complexity of the ^1H NMR spectra of the terpenes is readily overcome by the use of two-dimensional techniques at high magnetic field. Figure 16 depicts the 500 MHz spectrum of (-)-menthol itself, as well as those of the trichloroacetate ester and the arphos cluster, 29. The assignments were obtained using the two-dimensional NMR pulse sequence for the ^1H - ^1H COSY and the ^1H - ^{13}C shift-correlated experiments.³⁶ In the COSY experiment the data are presented as a contour map with the normal one-dimensional spectrum lying along the diagonal while proton resonances related by spin-spin couplings exhibit off-diagonal peaks. The COSY spectrum for $\text{Co}_3(\text{CO})_7(\text{arphos})\text{CCO}_2\text{-menthyl}$, 29, is shown in Figure 17. One can readily trace the coupling pattern of the protons around the menthyl ring and the complete ^1H and ^{13}C NMR chemical shift assignments are collected in Chapter Five.

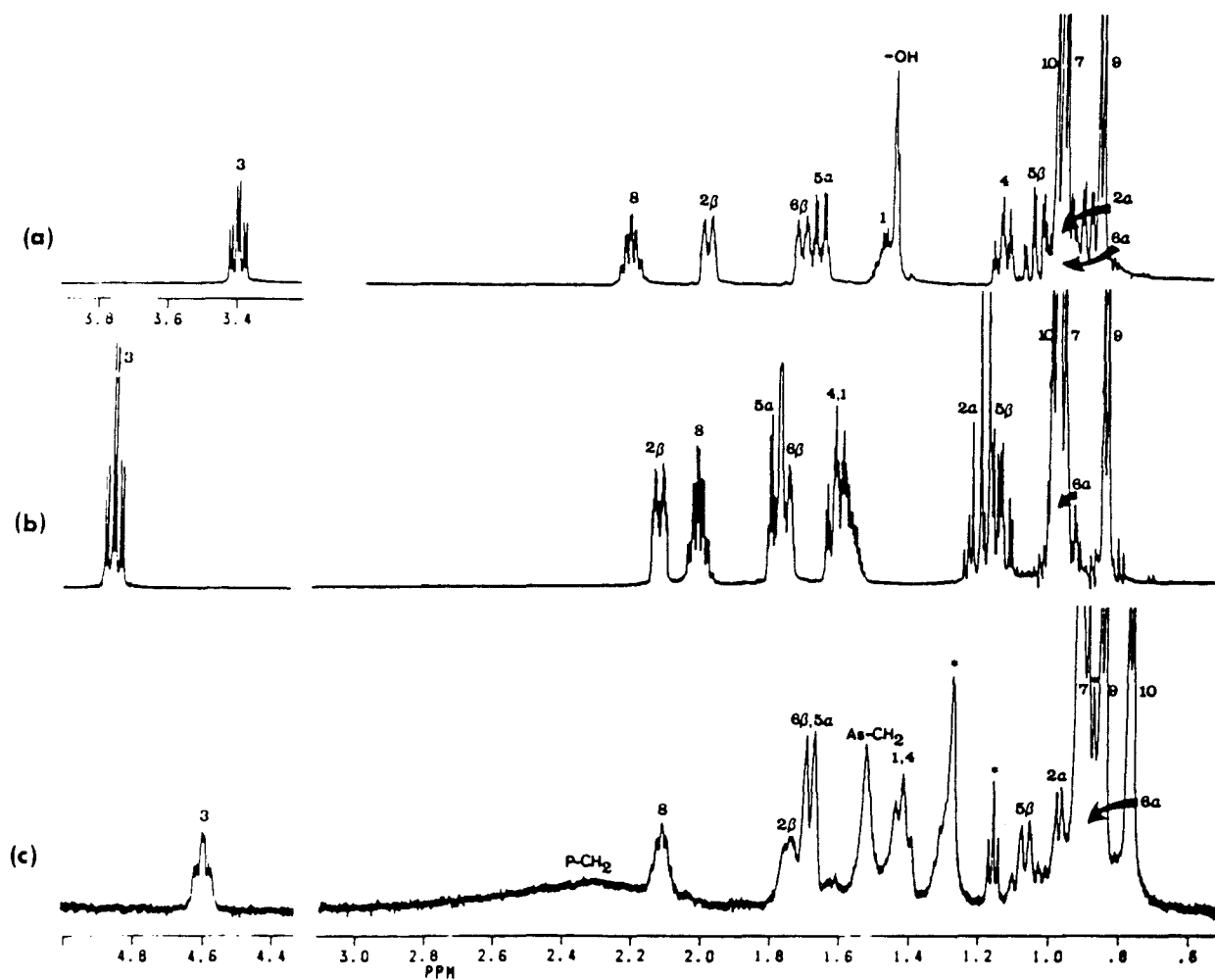


Figure 16 : 500 MHz ^1H NMR spectra (in CD_2Cl_2) of
 a) menthol, b) menthyl trichloroacetate, and
 c) $\text{Co}_3(\text{CO})_7(\text{arphos})\text{CCO}_2\text{menthyl}$, 29

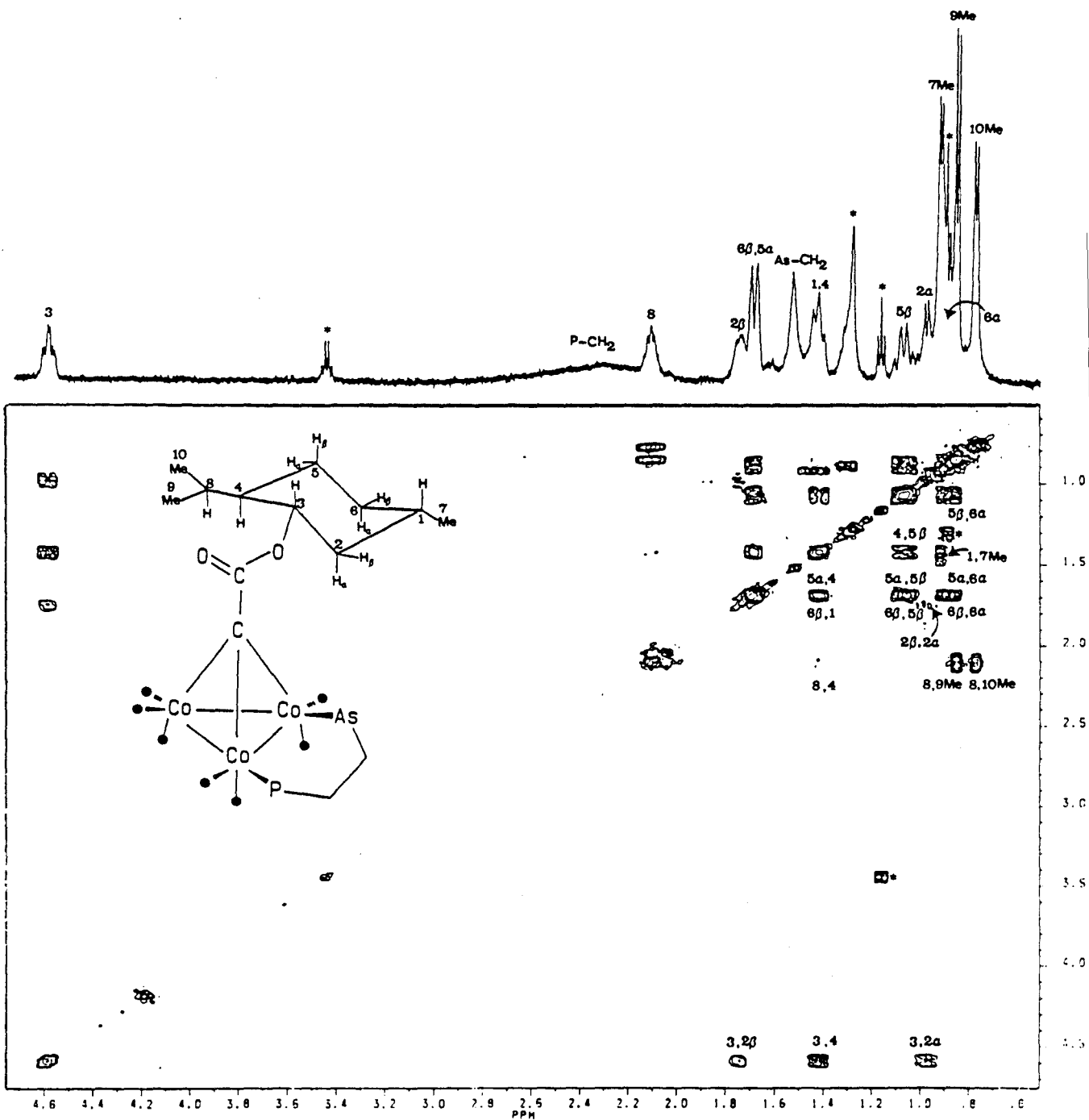
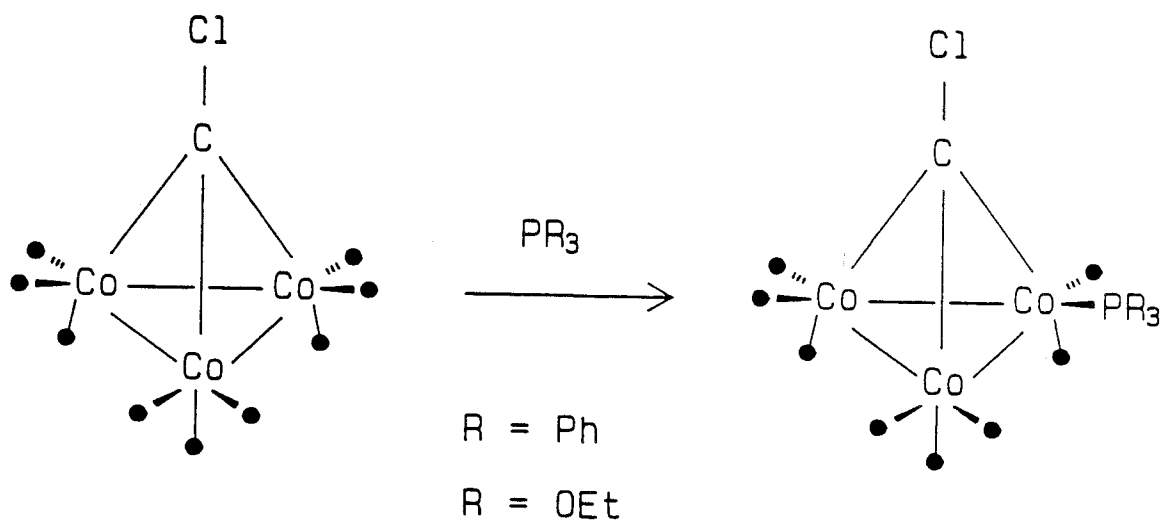


Figure 17 : 500 MHz two-dimensional ^1H - ^1H COSY NMR spectrum of $\text{CO}_3(\text{CO})_7(\text{arphos})\text{CCO}_2\text{menthyl}$, 29.

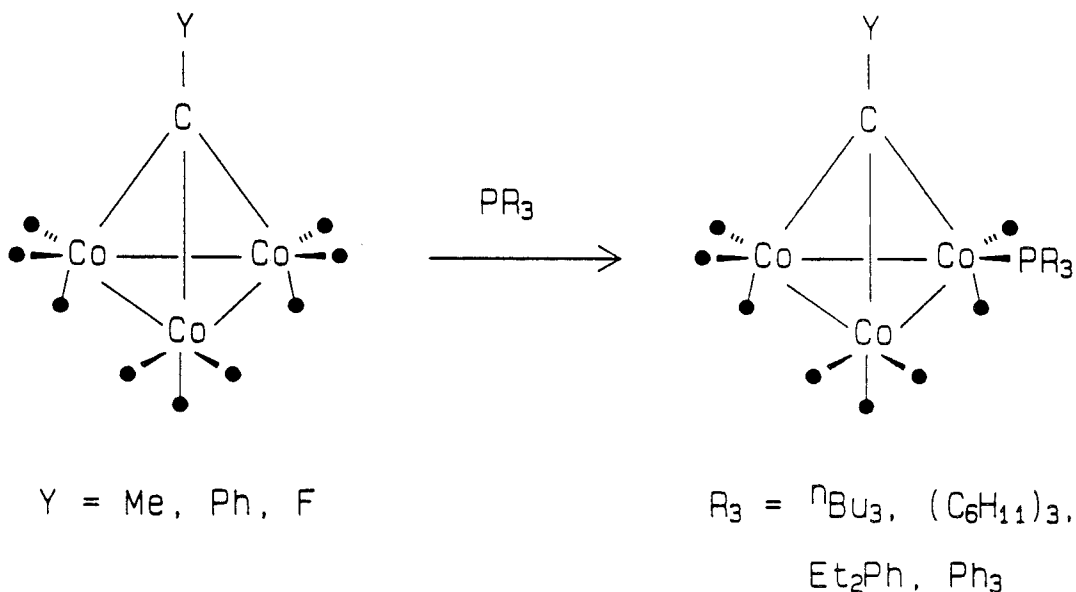
CHAPTER FOUR : REACTIONS OF CHIRAL MIXED METAL
CLUSTERS WITH MONOPHOSPHINES

4.1 Introduction

Tricobalt clusters are known to react with a wide variety of phosphines.^{30,37} Mono-substituted, air-stable derivatives, $R'CCo_3(CO)_8PR_3$, can be prepared by the direct reaction of the ligand and the cluster, at ambient or elevated temperatures. Aime³⁰ has prepared and characterized a number of substituted chloro clusters:



Robinson et al. have prepared phosphine-substituted clusters with a variety of different apical groups.³⁷ Substitution of an equatorial carbonyl is favoured in most cases.

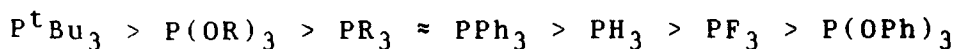


We wished to take advantage of this reactivity in our own research. The presence of a pair of diastereotopic cobalt vertices in a cluster suggests that it may be possible to bring about preferential attack at a single vertex. By replacing a $\text{Co}(\text{CO})_3$ unit by the isolobal fragment $\text{MoCp}(\text{CO})_2$ in the chiral clusters, a pair of diastereotopic cobalt vertices is created. To test the viability of observing chiral discrimination in these complexes, we treated them with a number of phosphines

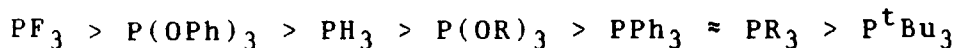
phosphorus.³⁸ This description is reminiscent of that used to describe the bonding of a carbonyl ligand to a metal. Molecular orbital theory has since been employed, using all of the σ and π orbitals of the appropriate symmetry on both the phosphine and the metal-containing moiety. The extent to which σ -bonding, π -bonding and steric factors affect the stability of the metal-phosphorus bond is listed in Table 1.³⁸

TABLE 1

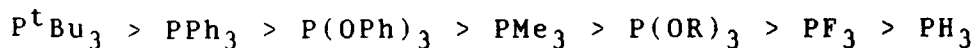
σ -bonding :



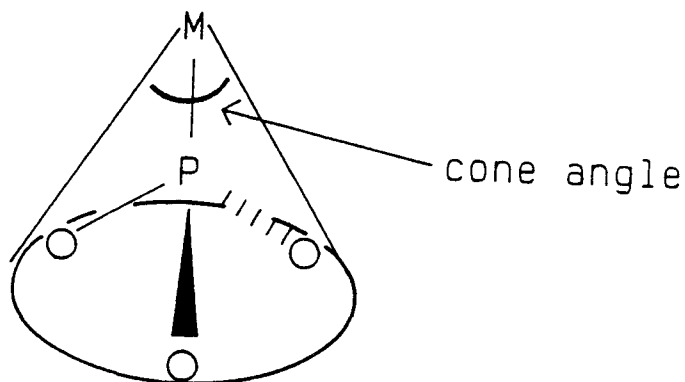
π -bonding :



Steric interference :



Steric factors have the most dominant effect on the metal-phosphorus bond, i.e., they can influence the course of a reaction most effectively.³⁸ The most commonly used measure of the size of a phosphine is Tolman's cone angle. This is defined as the angle at the metal atom of the cone swept out by the van der Waals' radii of the groups attached to the phosphorus atom.³⁸



The cone angles for some common phosphines are listed in Table 2.³⁸

Table 2 : Cone Angles for some Common Phosphines

<u>Ligand</u>	<u>Cone Angle °</u>
PH_3	87
$\text{P}(\text{OMe})_3$	107
$\text{P}(\text{OEt})_3$	109
PMe_3	118
PEt_3	132
PPh_3	145
PCy_3	171
P^tBu_3	182

It seemed likely that by varying the cone angle of the phosphines used to react with the chiral cluster, we could vary the degree of chiral discrimination observed.

To this end, we elected to work with three different ligands; these were trimethylphosphite, $\text{P}(\text{OMe})_3$, triphenylphosphine, PPh_3 , and tricyclohexylphosphine, PCy_3 .

4.2 Reactions of Mono-Phosphines with $\text{Co}_2(\text{CO})_6\text{MoCp}(\text{CO})_2$ CCO_2 -menthyl

All reactions were carried out by mixing the appropriate phosphine with the mixed metal cluster in tetrahydrofuran (THF). These reactions were not heated; rather all preparations were done at ambient temperature in order to favour the formation of the kinetic product rather than the thermodynamic one. It is the kinetic product that is the chirally discriminated one since this is the one produced via the pathway of lower activation energy.

The cluster 33 was allowed to react with one equivalent of trimethylphosphite. The resulting mixture of diastereomers exhibits two resonances in the P-31 NMR spectrum in approximately a 50/50 ratio (see Figure 18). This indicates that there was no chiral discrimination using the small $\text{P}(\text{OMe})_3$ ligand. It attacked both cobalt vertices with equal preference.

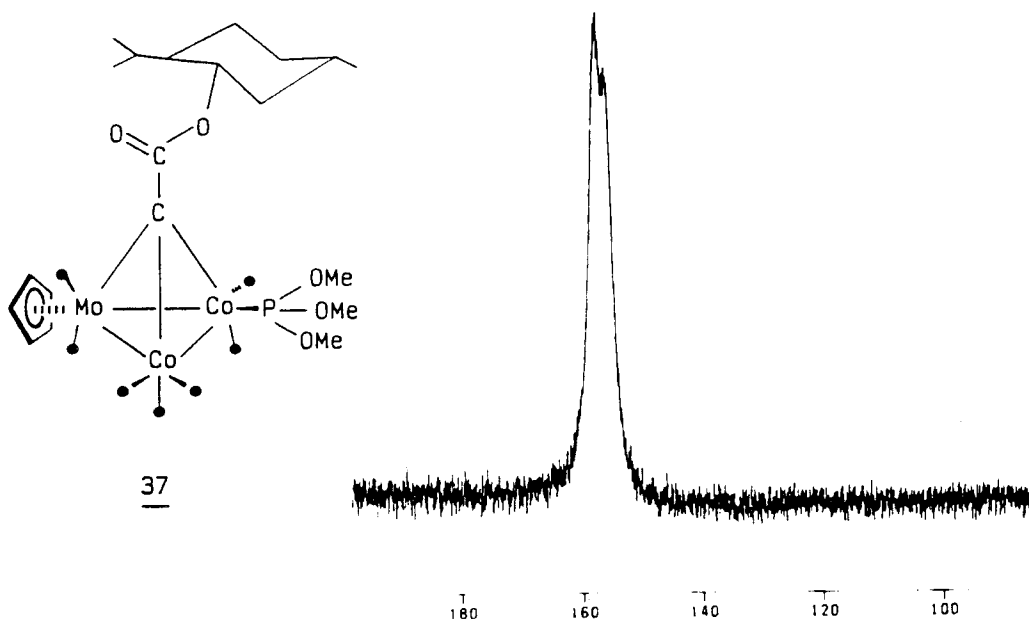


Figure 18 : 202.4 MHz ^{31}P NMR spectrum of $\text{Co}_2(\text{CO})_5[\text{P}(\text{OMe})_3]-\text{MoCp}(\text{CO})_2\text{CCO}_2\text{menthyl}$, 37, showing the $\approx 1 : 1$ ratio of diastereomers.

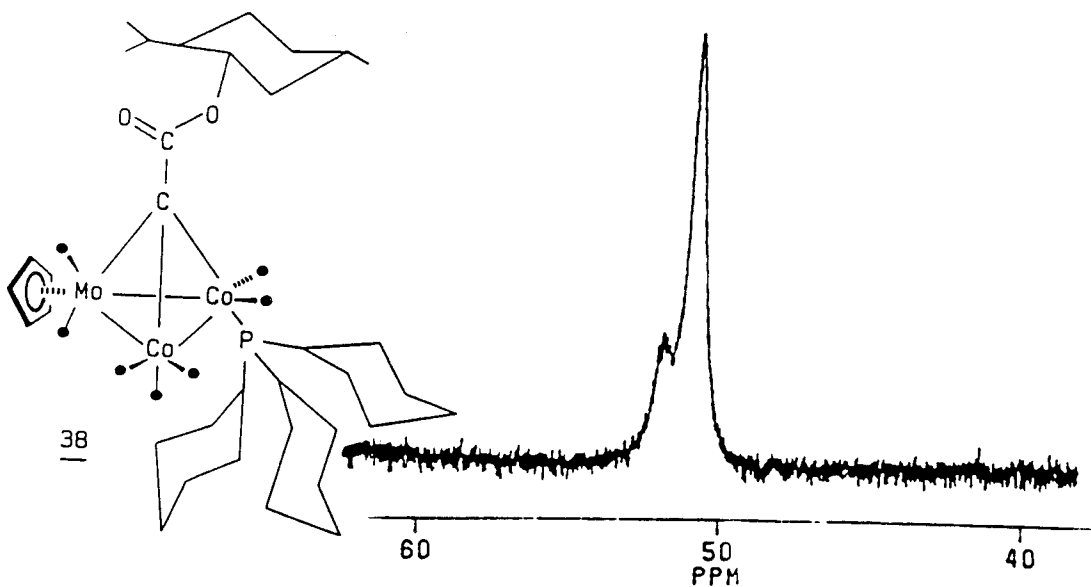


Figure 19 : 202.4 MHz ^{31}P NMR spectrum of $\text{Co}_2(\text{CO})_5[\text{P}(\text{C}_6\text{H}_{11})_3]-\text{MoCp}(\text{CO})_2\text{CCO}_2\text{menthyl}$, 38, showing the 1 : 3 ratio of diastereomers.

If the reaction were to proceed with any degree of selectivity, the phosphorus-31 NMR spectrum ought to show resonances of unequal intensity. The reaction of the cluster, 33, with tricyclohexylphosphine produced such results (see Figure 19). The 202.4 MHz P-31 spectrum of the cluster 38 shows two resonances in an integrated ratio of 75/25. Tricyclohexylphosphine has a cone angle of 171° , so it is not surprising that one was able to observe preferential attack at one cobalt over the other.

Treatment of the cluster 33 with triphenylphosphine produced unexpected results. Firstly, it was not possible to separate the phosphine bonded product from the reactant cluster by conventional chromatographic techniques. Preliminary tests indicate that reverse phase high pressure liquid chromatography could help to solve this problem in the future. However, this inability to separate the two clusters did not deter us. Since the selectivity was determined by P-31 NMR spectroscopy, the product did not have to be isolated from the reactant.

The phosphorus spectrum, surprisingly, showed only a single, sharp resonance at 28.0 ppm. There are two viable explanations for this observation. The first is that we have prepared a single optically pure product. However, the cone angle for PPh_3 is smaller than that for PCy_3 , so this argument remains unconvincing. The second

possibility is that two products are formed and each resonates at the same frequency. This seems the more probable explanation.

4.3 Reactions of Mono-Phosphines with $\text{Co}_2(\text{CO})_6\text{MoCp}(\text{CO})_2\text{C}-\text{CO}_2\text{-exo-bornyl}$

The preceding phosphine reactions were repeated using the *exo*-bornyl ester cluster, 34. The results were similar to those for the menthyl cluster, with a few minor differences.

The reaction with $\text{P}(\text{OMe})_3$ was done using a large excess of the phosphite. This is the only reaction with a monodentate ligand that went to completion, presumably because of the presence of excess phosphite. Two distinct products were observed by TLC. These were separated and determined to be the monosubstituted product, $\text{Co}_2(\text{CO})_5[\text{P}(\text{OMe})_3]\text{MoCp}(\text{CO})_2\text{-exo-bornyl}$, 39, and the disubstituted product, $\text{Co}_2(\text{CO})_4[\text{P}(\text{OMe})_3]_2\text{CCO}_2\text{-exo-bornyl}$, 40. The phosphorus NMR of the monosubstituted product showed only one fairly broad peak in the spectrum. It is not at all likely that only one optically pure product was obtained. Therefore, we conclude that attack was equally likely at both cobalt vertices and each product has the same P-31 chemical shift. To substantiate this conclusion, the P-31 NMR spectrum of the disubstituted product

was recorded. Again, only one broad peak was observed.

Treatment of the *exo*-bornyl cluster, 34, with tricyclohexylphosphine gave a P-31 spectrum showing three signals. There were two peaks at 55.1 and 56.2 ppm in a ratio of 55:45. These peaks are attributed to the phosphine-bonded clusters, which show some rather minimal chiral discrimination. The third resonance was a large, sharp peak at 50.7 ppm which can be attributed to the oxide of PCy₃ which shows a characteristic resonance at this chemical shift.

The cluster 34 was allowed to react with PPh₃ and again the product was inseparable from the reactant cluster. The P-31 NMR spectrum showed two peaks. There was an intense, sharp signal at 28.8 ppm and a small, broad peak at 45.6 ppm. Phosphine substitutions usually occur equatorially, but in some cases axial substitution has been reported.^{1a,39} This change from the equatorial to the axial position of the phosphine is usually associated with a downfield shift in the ³¹P NMR spectrum.⁴⁰ Therefore, the small peak at 45.6 ppm could be explained by the presence of a phosphine-substituted cluster in the axial position. This leaves only the one signal at 28.8 ppm to account for the equatorially bonded PPh₃ on the

cluster. As with the analogous menthyl complex, this peak could indicate 100 % chiral discrimination or, more likely, that there were two diastereomers synthesized, both of which have the same chemical shift.

4.4 Characterization of the Phosphine Substituted Clusters

All of the products prepared were characterized using the standard methods described earlier. Elemental analysis and IR spectroscopy were not carried out on the triphenylphosphine clusters, as these could not be separated from their precursors. However, FAB mass spectrometry did show the presence of these products conclusively. A typical FAB mass spectrum of a phosphine substituted cluster is shown in Figure 20.

4.5 Preparation of a Chiral Phosphine, $\text{PPh}_2(\text{neomenthyl})$

It was anticipated that use of a bulky and chiral phosphine would yield a single optically pure product when treated with a chiral dicobalt molybdenum cluster. To this end, we prepared (+)-neomenthyldiphenylphosphine from menthol and triphenylphosphine (see Scheme 3) by known procedures.^{41,42,43}

(+)-Neomenthyldiphenylphosphine, 41, was obtained as a white, crystalline, highly air sensitive solid.

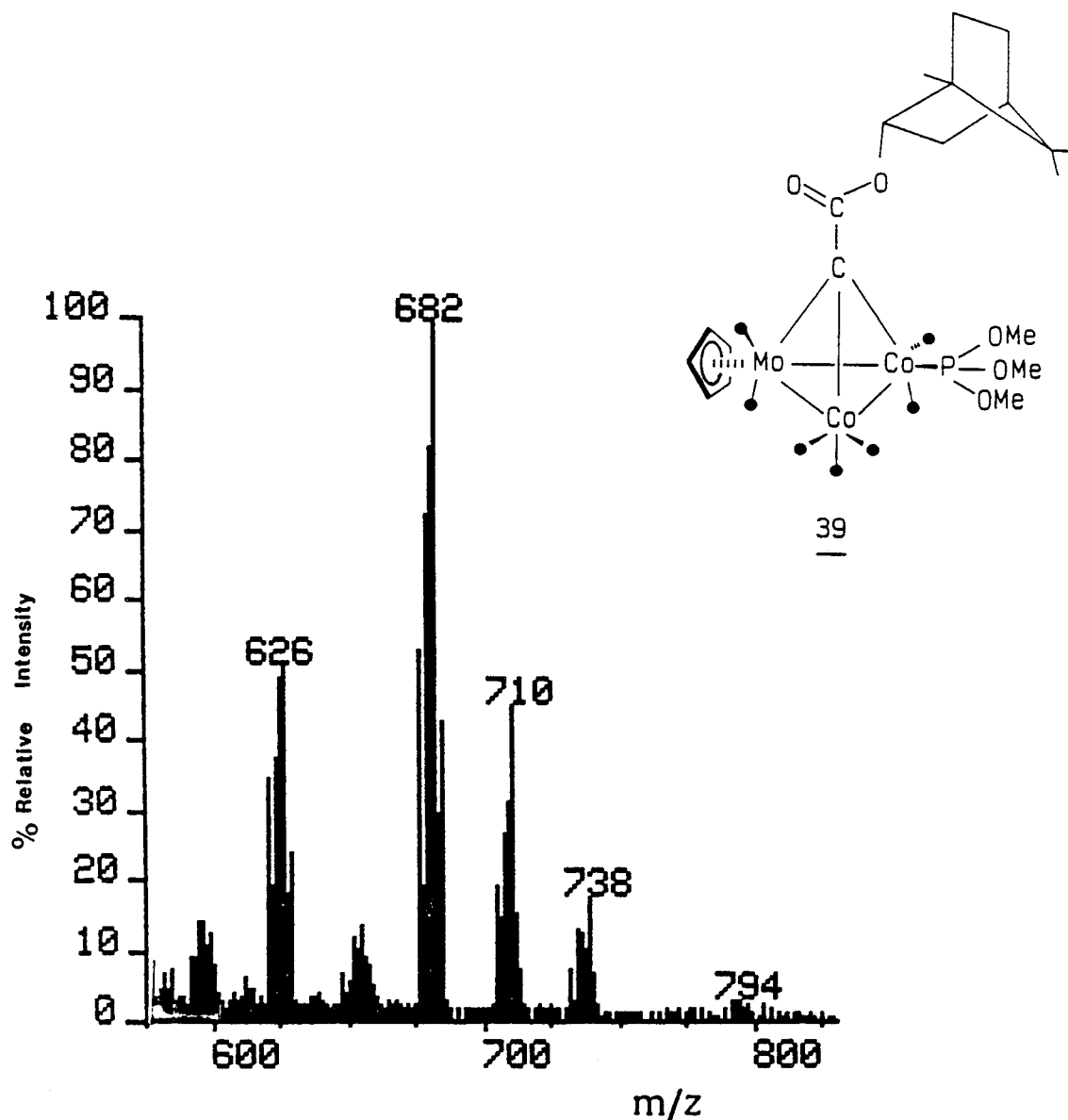
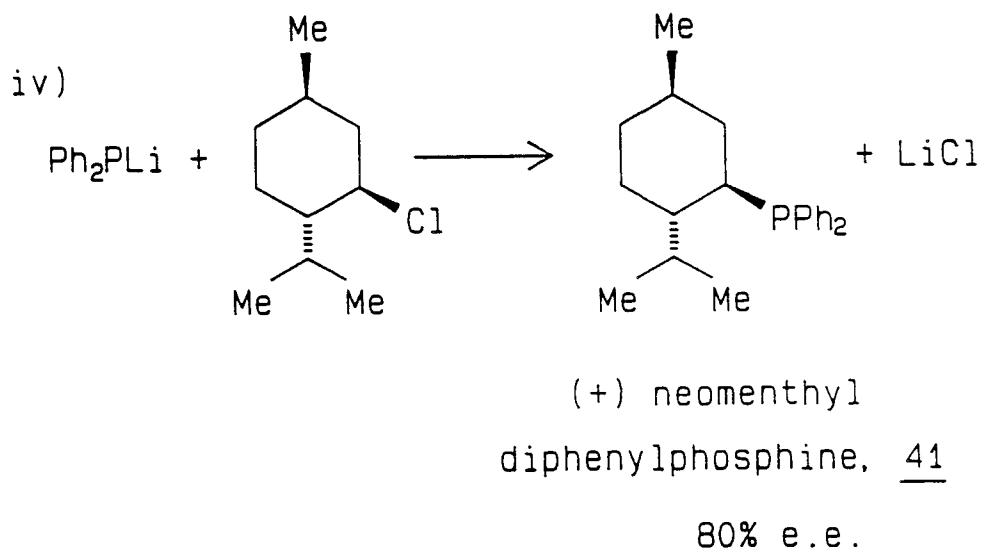
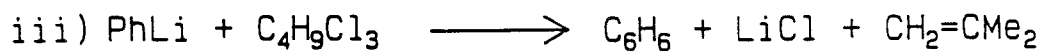
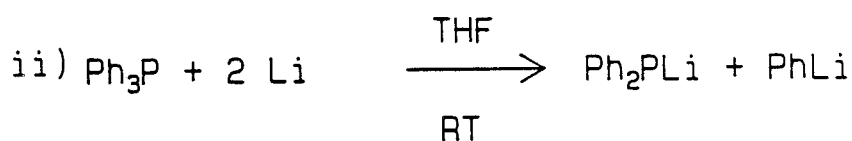
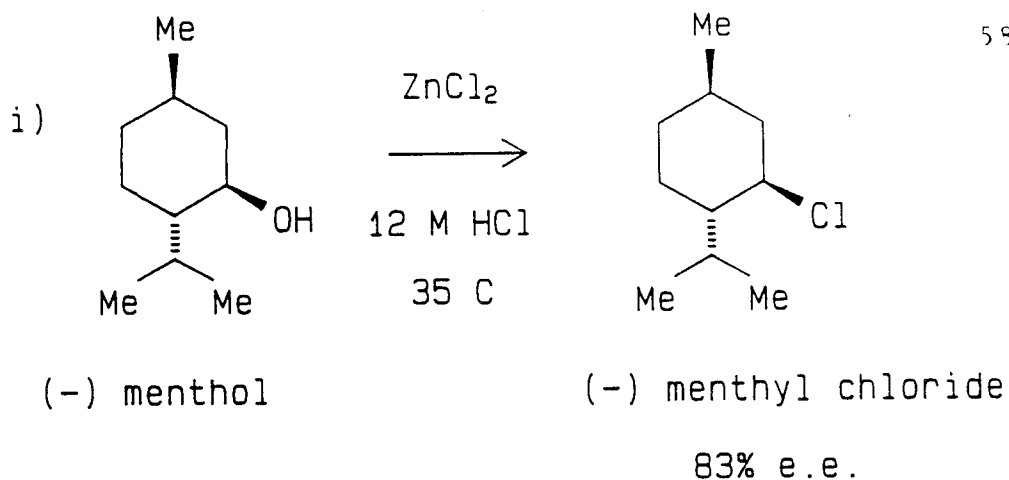


Figure 20 : High mass region of the FAB mass spectrum of $\text{Co}_2(\text{CO})_5[\text{P}(\text{OMe})_3\text{MoCp}(\text{CO})_2\text{CCO}_2\text{-exo-bornyl}]_2$, 39. The peak at m/z 794 corresponds to the M^+ ion.



Scheme 3 : Preparation of (+) Neomenthyldiphenylphosphine, 41.

4.6 Treatment of a Chiral Mixed Metal Cluster with a Chiral Phosphine

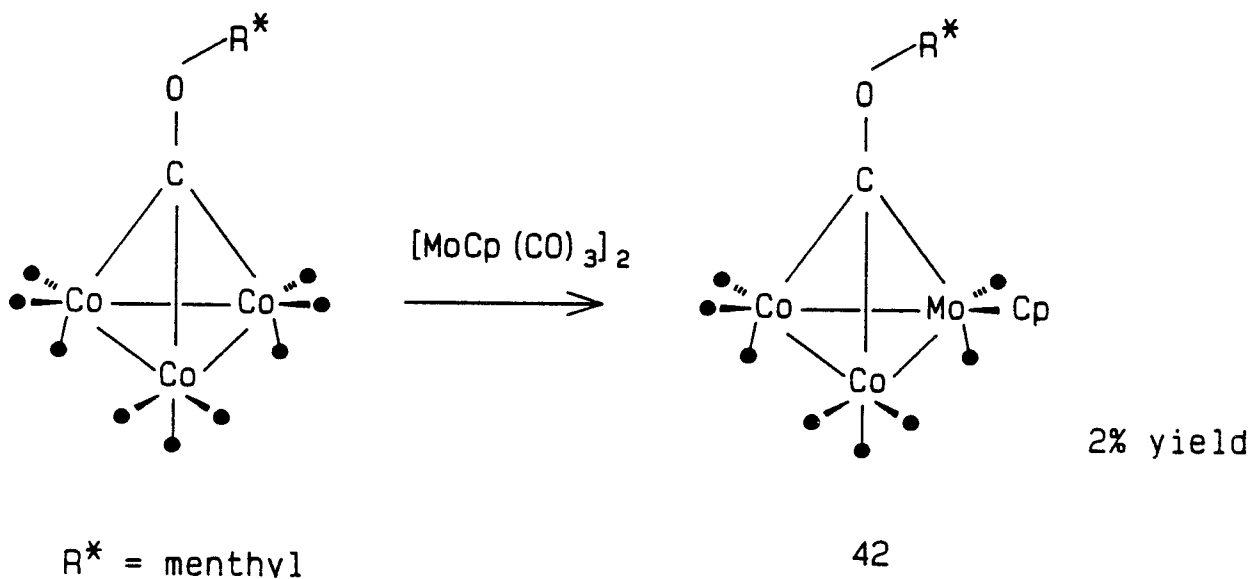
The menthyl mixed metal cluster 33 was treated with the chiral phosphine, 41. The phosphine-coordinated product was observed by TLC as a faint yellow-green spot at an R_f value slightly greater than the starting cluster. When isolation of this product was attempted by column chromatography, it decomposed. Unfortunately, the desired cluster was very air-sensitive.

The reaction was repeated with the intent of recording the P-31 NMR spectrum of the product without prior isolation from the starting material. However, during transfer of the product, it again decomposed, i.e., it was no longer visible by TLC. All transfers were carried out in a glove bag under a nitrogen atmosphere and evacuation of the solvent was done under vacuum. It is obvious that this product is extremely prone to decomposition and more effective dry box techniques must be employed if one hopes to study this system.

4.7 Related Work in this Area

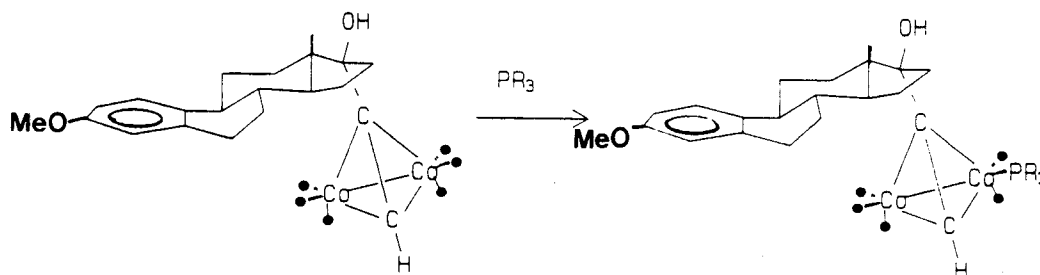
It was assumed that by bringing the chiral capping group closer to the diastereotopic cobalt atoms we could possibly attain 100 % chiral discrimination in reactions with mono-phosphines.³³ Preparation of a chiral tricobalt

ether cluster, 31, has already been discussed. It was necessary to substitute one of the $\text{Co}(\text{CO})_3$ units with the isolobal $\text{MoCp}(\text{CO})_2$ moiety in order to obtain two diastereotopic cobalt sites. It was found, however, that this substitution went in extremely poor yield, producing an unstable mixed metal cluster.³³ This cluster is probably sterically disfavoured as seems to be the case from its Chem-X model. This would account for both the low yield and the instability of the product.



As a result, this work was not pursued, i.e., treatment with phosphines was not attempted.

Present work in this area includes treatment of dicobalt steroidal clusters with phosphines, as in 43.⁴⁴

43

If preferential attack were to occur in any system it should be this one in which the chiral capping group is extremely bulky and is situated very close to the diastereotopic cobalt vertices. Notice that there is neither an ester nor an ether fragment separating the apical group from the cluster. This area of study is now in progress.

4.8 Conclusion

To conclude, it has been shown that chiral tetrahedral clusters containing three metal vertices can be obtained by incorporating a terpenoidal fragment at the apical position, viz., menthyl or *exo*-bornyl. This chirality can be detected using a number of effective probes. These include the use of bidentate ligands such as arphos and diphos and also substitution of a $\text{Co}(\text{CO})_3$ unit by the $\text{Mo}(\eta^5\text{Cp-R})(\text{CO})_2$ fragment, where R is the probe. Furthermore, these mixed metal species contain two diastereotopic cobalt nuclei. It has been shown that the presence of a bulky chiral substituent at the apical position of the cluster can induce preferential attack of a phosphine at one cobalt over the other.

CHAPTER FIVE : EXPERIMENTAL

5.1 General Spectroscopic Techniques

NMR spectra were obtained using a Bruker AM 500 or a WM 250 spectrometer. ^1H and ^{13}C chemical shifts are reported relative to tetramethylsilane; ^{31}P chemical shifts are quoted relative to 85% H_3PO_4 . Infrared spectra were recorded on a Perkin-Elmer 283 instrument using NaCl plates. Fast atom bombardment (FAB) mass spectra were obtained on a VG analytical ZAB-SE spectrometer with an accelerating potential of 8 kV and a resolving power of 10,000. NBA was used as the sample matrix and Xe as the bombarding gas.

5.2 General Procedures

All preparations were carried out under an atmosphere of dry nitrogen employing conventional benchtop and glovebag techniques. Solvents were dried according to standard procedures before use.⁴⁵ Silica gel (Merck 9385, particle size 20-40 μ) was employed for flash chromatography.

Microanalytical data were obtained for all new compounds from the Guelph Chemical Laboratories, Guelph, Ontario.

5.3 Experimental Procedures

Preparation of $\text{Co}_3(\text{CO})_9\text{CCO}_2$ menthyl, 15

The tricobalt cluster, 15, was prepared by the method of Vahrenkamp.²² A solution of $\text{Co}_2(\text{CO})_8$ (13.863 g, 40.5 mmol) and menthyl trichloroacetate (6.789 g, 22.5 mmol) in THF (120 mL) was stirred at reflux for four hours. The progress of the reaction was followed by TLC on Kieselgel (eluent, ether/hexane, 20/80) which revealed the formation of 15 (R_f 0.86) as a dark purple spot. The mixture was cooled to room temperature and the cobalt salts removed by filtration. The filtrate was evaporated to dryness and the crude product was extracted with hexane. The hexane extracts were combined and the solvent removed by roto-evaporation. The resulting red-purple oil was filtered through silica gel (eluent, CH_2Cl_2 /hexane, 1/3) to give dark purple crystals of 15 (6.757 g, 10.83 mmol, 48%).

Preparation of $\text{Co}_3(\text{CO})_9\text{CCO}_2$ -*exo*-bornyl, 16

The cluster, 16, was prepared in the same manner as 15. *Exo*-bornyl trichloroacetate was used in place of the

menthyl derivative. The reaction was monitored by TLC on Kieselgel (eluent, ether/hexane, 20/80) which revealed formation of 16 as a dark purple spot at R_f 0.90. The product was obtained as a deep red-purple oil, even after filtration through silica gel (eluent, CH_2Cl_2 /hexane, 1/3). The oil was dissolved in hexane and the solvent evaporated by passing a slow stream of N_2 gas over the solution. A dark red crystalline solid, 16, was obtained (2.919 g, 4.69 mmol, 26 %). ^{13}C NMR (C_6D_6) δ 199.1 [cobalt carbonyls], 83.4 [C-2], 45.3 [C-4], 39.1 [C-3], 34.2 [C-6], 27.2 [C-5], 20.2 [C-8, C-9], 11.7 [C-10]. Signals for the quaternary carbons 1 and 7 were not observed. IR (CH_2Cl_2) ν_{CO} 2110(m), 2065(vs), 2060(vs), 2040(vs), 1670(ester) cm^{-1} . FAB mass spectrum : m/z (%) 622(5) (M^+); 594(100) ($\text{M}-\text{CO}^+$); 566(2) ($\text{M}-2\text{CO}^+$); 538(25) ($\text{M}-3\text{CO}^+$); 510(78) ($\text{M}-4\text{CO}^+$); 482(22) ($\text{M}-5\text{CO}^+$); 454(2) ($\text{M}-6\text{CO}^+$); 426(5) ($\text{M}-7\text{CO}^+$). Anal. Calcd. for $\text{C}_{21}\text{H}_{17}\text{O}_{11}\text{Co}_3$: C, 40.54; H, 2.75. Found : C, 40.47; H, 2.91.

Preparation of menthyl trichloroacetate, $\text{C}_{10}\text{H}_{19}\text{CO}_2\text{CCl}_3$

Menthol (20.331 g, 130 mmol) was dissolved in ether (40 mL) and 11 mL of pyridine was added. Trichloroacetylchloride (24.843 g, 136 mmol) was dissolved in ether (25 mL) and added dropwise to the menthol/ pyridine solution over a period of 45 minutes. A white solid

(pyridine/HCl salt) appeared immediately. The reaction was stopped when the formation of this salt had subsided. Pyridine was added to the reaction mixture until the pH was neutral. Ether (35 mL) was added to the mixture. It was then extracted with 1.2 M HCl (1x100 mL, 2x75 mL). The water layers were combined and extracted with ether (2x50 mL). The ether layers were combined and dried over anh. Na_2SO_4 . The solution was filtered and the solvent removed by roto-evaporation, leaving a slightly yellow liquid, menthyl trichloroacetate (38.165 g, 127 mmol, 97 %). The liquid solidified on refrigeration. ^1H NMR (CD_2Cl_2) δ 4.83 (1H) [H-3], 2.17 (1H) [H-2 β], 2.0 (1H) [H-8], 1.79 (1H) [H-5 α], 1.75 (1H) [H-6 β], 1.60 (1H) [H-4 α], 1.58 (1H) [H-1 β], 1.19 (1H) [H-2 α], 1.16 (1H) [H-5 β], 0.96 (4H) [H-6 α , Me-10], 0.94 (3H) [Me-7], 0.82 (3H) [Me-9].

Preparation of *exo*-bornyl trichloroacetate, $\text{C}_{10}\text{H}_{17}\text{CO}_2\text{CCl}_3$

The trichloroacetate was prepared in quantitative yield in the same manner as the menthyl analogue. ^{13}C NMR (C_6D_6) δ 160.8 [ester carbonyl], 86.2 [C-2], 65.6 [C-Cl $_3$], 49.0 [C-1], 46.6 [C-7], 44.6 [C-4], 37.6 [C-3], 32.9 [C-6], 26.5 [C-5], 19.6 [C-9], 19.4 [C-8], 10.8 [C-10].

Preparation of $[\text{Mo}(\text{CO})_3(\text{i-Pr-Cp})]_2$, 20

The dimer, 20, was prepared by the method of Abel et al.²⁸ $\text{Mo}(\text{CO})_6$ (5.992 g, 22.7 mmol) and 6,6-dimethylfulvene (3.609 g, 34.1 mmol) were stirred at reflux in high boiling petroleum ether for 6 h. The reaction mixture became deep red in colour. The solution was cooled to room temperature and the volatile materials removed using the vacuum line and heating to 60°C. A red residue remained. This was filtered through alumina gel (eluent, hexane) and the red band collected, yielding fine red crystals of 20 (2.490 g, 4.3 mmol, 38 %). ^{13}C NMR (CD_2Cl_2) δ 94.5, 88.9 [Cp-CH's], 28.0 [Cp-CHMe₂], 23.9 [Cp-CHMe₂]. FAB mass spectrum : m/z (%) 575(14) (M+1)⁺; 546(15) (M-CO)⁺; 518(88) (M-2CO)⁺; 490(45) (M-3CO)⁺; 462(57) (M-4CO)⁺; 434(25) (M-5CO)⁺.

Preparation of 6,6-dimethylfulvene

Dimethylfulvene was prepared by the method of Crane et al.²⁷ Freshly cracked cyclopentadiene (40.095 g, 0.608 mol) and acetone (35.235 g, 0.608 mol) were stirred together in a round bottomed flask fitted with a reflux condenser in an ice bath. To this was added dropwise 12 mL of 20 % KOH/EtOH solution. The reaction mixture became a dark amber colour. The water layer was separated from the organics, and the organic layer vacuum distilled. The product was obtained as a pale yellow liquid (19.504 g, 0.184 mol,

30 %): bp 25°C, 3.5 mm Hg; ^1H NMR (CDCl_3) δ 6.40 (s, 4H) [Cp ring protons], 2.17 (s, 6H) [methyl protons].

Preparation of $[\text{Mo}(\text{CO})_3(\text{C}_9\text{H}_7)]_2$, 21

The dimer, 21, was prepared by the method of King et al.²⁹ $\text{Mo}(\text{CO})_6$ (6.428 g, 24.3 mmol) and indene (5.649 g, 48.7 mmol) were stirred at reflux in high boiling petroleum ether (30 mL) for 16 h. The reaction mixture became dark brown. The solution was cooled to room temperature and filtered under vacuum. The resulting brown solid was sublimed to remove the volatile $\text{Mo}(\text{CO})_6$. The product was obtained as a fine dark brown powder (0.9469 g, 1.6 mmol, 13 %). ^{13}C NMR (CD_2Cl_2) δ 126.1, 124.2 [indenyl aromatic carbons], 93.4 [indenyl C-2], 84.1 [indenyl C-1, C-3]. FAB mass spectrum : m/z (%) 538(10) ($\text{M}-2\text{CO}$)⁺; 479(10) ($\text{M}-\text{C}_9\text{H}_7$)⁺; 423(100) ($\text{M}-2\text{CO}-\text{C}_9\text{H}_7$)⁺; 395(9) ($\text{M}-3\text{CO}-\text{C}_9\text{H}_7$)⁺.

Preparation of $(i\text{-Pr-C}_5\text{H}_4)\text{MoCo}_2(\text{CO})_8\text{CCO}_2\text{menthyl}$, 22

$[\text{Mo}(\text{CO})_3(i\text{-Pr-Cp})]_2$ (0.3707 g, 0.64 mmol) and 15 (0.6573 g, 1.05 mmol) were heated under reflux in THF (35 mL) for 18 hours. Progress of the reaction was followed by TLC on Kieselgel (eluent, ether/hexane, 4/96) showing a dark green spot, 22, at R_f 0.31. This green band was collected by flash chromatography on silica gel (eluent, ether/hexane, 3/97) yielding a dark green oil, 22, which solidified on standing at room temperature (0.2881 g, 0.39

mmol, 37%): dec > 170°C; ^{13}C NMR (CD_2Cl_2) δ 210 broad [exchanging molybdenum and cobalt carbonyls], 180.0 [ester carbonyl], 93.2, 89.1 [Cp-CH's], 75.5 [C-3], 47.2 [C-4], 41.0 [C-2], 34.3 [C-6], 31.4 [C-1], 28.0 [Cp-CHMe₂], 27.5 [Cp-CHMe], 26.0 [C-8], 23.3 [Cp-CHMe], 23.2 [C-5], 21.7 [C-7], 21.4 [C-10], 15.3 [C-9]; IR(CH_2Cl_2) ν_{CO} 2090(m), 2080(m), 2035(vs), 2025(vs), 2010(vs), 1995(sh), 1920(m), 1850(m), 1730(w), 1660(ester) cm^{-1} . FAB mass spectrum: m/z (%) 801(13) ($\text{M}+2\text{CO}$)⁺; 772(34) ($\text{M}+\text{CO}$)⁺; 742(68) (M)⁺; 714(32) ($\text{M}-\text{CO}$)⁺; 686(62) ($\text{M}-2\text{CO}$)⁺; 658(36) ($\text{M}-3\text{CO}$)⁺; 630(60) ($\text{M}-4\text{CO}$)⁺; 602(50) ($\text{M}-5\text{CO}$)⁺; 574(100) ($\text{M}-6\text{CO}$)⁺; 546(58) ($\text{M}-7\text{CO}$)⁺. Anal. Calcd. for $\text{C}_{28}\text{H}_{30}\text{O}_{10}\text{Co}_2\text{Mo}$: C, 45.42; H, 4.08. Found: C, 45.30; H, 3.92.

Preparation of $(\text{C}_9\text{H}_7)\text{MoCo}_2(\text{CO})_8\text{CCO}_2\text{menthyl}$, 23

[$\text{Mo}(\text{CO})_3(\text{C}_9\text{H}_7)$]₂, 21 (0.5381 g, 0.912 mmol) and 15 (0.7726 g, 1.24 mmol) were heated under reflux in THF (35 mL) for 14 hours and then stirred at ambient temperature for 24 hours. The reaction was followed by TLC on Kieselgel, showing the formation of a green product 23 at R_f 0.29 (eluent, ether/hexane, 5/95). The solvent was removed leaving a brown residue. Flash chromatography (eluent, ether/hexane, 5/95) yielded a dark green oil which solidified on standing at room temperature (0.1766 g, 0.24 mmol, 19%): dec 155°C; ^{13}C NMR (CD_2Cl_2) δ 210 broad [exchanging molybdenum and cobalt carbonyls], 127.5, 124.1

[indenyl aromatic CH's], 92.8, [indenyl C-2], 84.0, 82.1 [indenyl C-1, C-3], 75.7 [C-3], 47.4 [C-4], 41.2 [C-2], 34.2 [C-6], 31.7 [C-1], 25.8 [C-8], 23.0 [C-5], 21.8 [C-7], 20.8 [C-10], 15.6 [C-9]; IR(CH₂Cl₂) ν_{CO} 2080(m), 2070(w), 2045(s), 2020(s), 2000(s), 1945(w), 1895(w), 1720(m), 1740(sh), 1660(ester) cm⁻¹. FAB mass spectrum: *m/z* (%) 750.82(16) (M)⁺; 692(7) (M-2CO)⁺; 666(11) (M-3CO)⁺; 638(9) (M-4CO)⁺; 610(42) (M-5CO)⁺; 582(100) (M-6CO)⁺; 554(51) (M-7CO)⁺. Anal. Calcd. for C₂₉H₂₆O₁₀Co₂Mo: C, 46.55; H, 3.50. Found: C, 46.27; H, 3.26.

Preparation of (C₉H₇)MoCo₂(CO)₆(arphos)CCO₂menthyl, 24/25

A solution of 23 (0.1766 g, 0.24 mmol) and arphos (0.0870 g, 0.20 mmol) in THF (20 mL) was stirred at ambient temperature for 10 minutes and then at reflux for 40 minutes. The progress of the reaction was monitored by TLC on Kieselgel (eluent, ether/hexane, 5/95), showing a yellow-green spot, 24/25 at R_f 0.10. Chromatography on alumina gel (eluent, ether/hexane, 20/80) yielded dark green crystals, 24/25 (0.1368 g, 0.12 mmol, 61%): dec 118-120°C; ¹³C NMR (CD₂Cl₂) δ 211 broad [exchanging molybdenum and cobalt carbonyls], 181.8 [ester carbonyl], 141-124 [phenyls and indenyl aromatic CH's], 94.2/93.7 [indenyl C-2], 84.7/84.5, 82.5/82.3 [indenyl C-1, C-3], 75.2 [C-3], 47.6/47.1 [C-4], 41.5/41.1 [C-2], 34.8 [C-6], 32.0 [C-1],

26.0/25.9 [C-8], 25.4 [CH₂-P], 23.7 [CH₂-As], 23.2 [C-5], 22.3 [C-7], 20.8 [C-10], 16.3 [C-9]; ³¹P NMR (CD₂Cl₂) [300 K] 43.5 and 42.0 ppm; IR(CH₂Cl₂) ν_{CO} 2030(w), 2010(m), 1985(vs), 1975(vs), 1945(m), 1910(m), 1740(sh), 1720(s), 1635(ester) cm⁻¹. FAB mass spectrum: *m/z* (%) 1052(37) (M-3CO)⁺; 1024(100) (M-4CO)⁺; 996(7) (M-5CO)⁺; 968(6) (M-6CO)⁺. Anal. Calcd. for C₅₃H₅₀O₈Co₂MoAsP: C, 56.10; H, 4.44. Found: C, 56.36; H, 4.48.

Preparation of (Ph₂PCH₂CH₂PPh₂)Co₃(CO)₇CCO₂menthyl, 28

A solution of 15 (1.030 g, 1.65 mmol) and diphos (0.6396 g, 1.61 mmol) in THF (65 mL) was stirred at reflux for 10 minutes and then at room temperature for a further 30 minutes. The reaction was monitored by TLC on Kieselgel (eluent, ether/hexane, 20/80) which showed the formation of 28 as a green spot (R_f 0.10). Chromatography on silica gel (eluent, ether/hexane, 20/80) gave dark green crystals of 28 (0.5135 g, 0.53 mmol, 33 %): mp 85-87°C; ¹³C NMR (CD₂Cl₂) δ 205.2 [cobalt carbonyls], 182.1 [ester carbonyl], 132.8, 131.2, 130.2, 128.6 [phenyl carbons], 74.9 [C-3], 47.7 [C-4], 41.3 [C-2], 34.6 [C-6], 31.8 [C-1], 25.8 [C-8], 25.4 [CH₂-P], 23.1 [C-5], 22.0 [C-7], 20.8 [C-10], 15.8 [C-9]; ³¹P NMR (CD₂Cl₂) [306 K] 49.3 and 46.8 ppm. IR(CH₂Cl₂) ν_{CO} 2050(s), 2000(vs), 1985(sh), 1960(sh), 1645(ester) cm⁻¹. FAB mass spectrum: *m/z* (%) 938(2)

$(M-CO)^+$; 882(41) $(M-3CO)^+$; 854(4) $(M-4CO)^+$; 826(21)
 $(M-5CO)^+$; 798(26) $(M-6CO)^+$; 771(21) $(M-7CO)^+$; 643(11)
 $(C_{29}H_{24}O_2Co_3P_2)^+$; 616(100) $(C_{28}H_{25}OCo_3P_2)^+$; 588(85)
 $(C_{27}H_{25}Co_3P_2)^+$; 560(27) $(C_{25}H_{21}Co_3P_2)^+$; 482(24)
 $(C_{19}H_{15}Co_3P_2)^+$; 406(58) $(C_{13}H_{11}Co_3P_2)^+$; 328(25)
 $(C_7H_5Co_3P_2)^+$. Anal. Calcd. for $C_{45}H_{43}O_9Co_3P_2$: C, 55.92;
 H, 4.69. Found: C, 55.70; H, 4.44.

Preparation of $(Ph_2AsCH_2CH_2PPh_2)Co_3(CO)_7CCO_2menthyl, 29$

A solution of 15 (0.4429 g, 0.71 mmol) and arphos (0.2862 g, 0.65 mmol) in THF (35 mL) was stirred at 40°C for 15 minutes and then at room temperature for a further 30 minutes. The progress of the reaction was followed by TLC on Kieselgel (eluent, ether/hexane, 15/85) which revealed the formation of 29 (R_f 0.39) as a dark green spot. Flash chromatography on silica gel (eluent, ether/hexane, 15/85) gave dark green crystals of 29 (0.4524 g, 0.45 mmol, 69%): mp 81-84°C; 1H NMR (CD_2Cl_2) δ 7.6-7.4 (20H) [phenyls], 4.6 (1H) [H-3], 2.3 broad (2H) [P-CH₂], 2.1 (1H) [H-8], 1.75 (1H) [H-2 β], 1.7 (2H) [H-6 β , H-5 α], 1.55 (2H) [As-CH₂], 1.4 (2H) [H-1 β , H-4 α], 1.1 (1H) [H-5 β], 1.0 (1H) [H-2 α], 0.95 (3H) [Me-7], 0.9 (1H) [H-6 α], 0.9 (3H) [Me-9], 0.8 (3H) [Me-10]; ^{13}C NMR (CD_2Cl_2) δ 204.7 [cobalt carbonyls], 131.7, 130.1, 129.8, 129.7, 128.8, 128.6, 128.5 [phenyl carbons], 74.7 [C-3], 47.5 [C-4], 41.0

[C-2], 34.4 [C-6], 31.6 [C-1], 25.7 [C-8], 25.6 [CH₂-P], 22.9 [C-5], 21.9 [C-7], 21.0 [C-10], 20.7 [CH₂-As], 15.7 [C-9]; ³¹P NMR (CD₂Cl₂) [300 K] 47.2 ppm; [193 K] 51.0 and 46.9 ppm. IR(CH₂Cl₂) ν_{CO} 2050(s), 2005(vs), 1980(sh), 1960(sh), 1640(ester) cm⁻¹. FAB mass spectrum: *m/z* (%) 982(5) (M-CO)⁺; 926(60) (M-3CO)⁺; 899(8) (M-4CO)⁺; 870(23) (M-5CO)⁺; 842(16) (M-6CO)⁺; 815(28) (M-7CO)⁺; 687(15) (C₂₉H₂₄O₂Co₃PAs)⁺; 660(100) (C₂₈H₂₅OCo₃PAs)⁺; 631(37) (C₂₇H₂₄Co₃PAs)⁺; 604(72) (C₂₅H₂₁Co₃PAs)⁺; 526(65) (C₁₉H₁₅Co₃PAs)⁺; 450(74) (C₁₃H₁₁Co₃PAs)⁺; 372(37) (C₇H₅Co₃PAs)⁺. Anal. Calcd. for C₄₅H₄₃O₉Co₃PAs: C, 53.49; H, 4.29. Found: C, 53.59; H, 4.16.

Preparation of (Ph₂AsCH₂CH₂PPh₂)Co₃(CO)₇CCO₂exo-bornyl, 30

The arphos cluster, 30, was prepared in the same manner as its menthyl analogue, 29. The progress of the reaction was followed by TLC on Kieselgel (eluent, ether/hexane, 20/80) which revealed the formation of 30 as a dark green spot (R_f 0.48). Flash chromatography on silica gel (eluent, ether/hexane, 15/85) gave dark green crystals of 30 (0.5128 g, 0.51 mmol, 88 %). ³¹P NMR (CH₂Cl₂) [293 K] 48.1 ppm; [178 K] 50.2 and 48.4 ppm; IR (CH₂Cl₂) ν_{CO} 2060(s), 2008(vs), 2006(vs), 1985(m), 1978(m), 1955(sh), 1640(ester) cm⁻¹; FAB mass spectrum : *m/z* (%) 1009(4) (M+1)⁺; 980(19) (M-CO)⁺; 924(100) (M-3CO)⁺; 896(10)

(M-4CO)⁺; 868(30) (M-5CO)⁺; 840(14) (M-6CO)⁺; 812(34)
 (M-7CO)⁺. Anal. Calcd. for C₄₅H₄₁O₉Co₃ASP : C, 53.59; H,
 4.10. Found : C, 53.42; H, 4.06.

Preparation of CpMoCo₂(CO)₈CCO₂menthyl, 33

The mixed metal cluster, 33, was prepared by the method of Vahrenkamp.²² A solution of 15 (1.993 g, 3.2 mmol) and [CpMo(CO)₃]₂ (1.178 g, 2.4 mmol) was stirred at reflux in THF (65 mL) for 11 h, followed by stirring at ambient temperature for 17 h. The reaction was followed by TLC on Kieselgel (eluent, ether/hexane, 15/85). A dark green spot at R_f 0.23 indicated the formation of the product, 33. Flash chromatography on silica (eluent, ether/hexane, 4/96) yielded the desired product, 33, as a green crystalline solid (1.141 g, 1.63 mmol, 51 %).

Preparation of CpMoCo₂(CO)₈CCO₂exo-bornyl, 34

The cluster, 34, was prepared in the same fashion as its menthyl counterpart, 33. The tricobalt species, 16, (1.30 g, 2.0 mmol) and the dimer [CpMo(CO)₃]₂ (0.880 g, 1.8 mmol) were stirred together at reflux in THF (35 mL) for 6 hours. The solution was then left at room temperature overnight. The progress of the reaction was monitored using TLC (eluent, ether/hexane, 20/80) showing a dark green spot at R_f 0.25. Flash chromatography (eluent, ether/

hexane, 7/93) yielded the product as a dark green oil which solidified on standing at room temperature (0.435 g, 0.62 mmol, 31 %). ^{13}C NMR (C_6D_6) δ 251.0 [apical C], 208.1 broad [exchanging molybdenum and cobalt carbonyls], 180.4 [ester carbonyl], 92.8, 92.7, 92.6 [Cp CH's], 83.8 [C-2], 46.3 [C-1], 44.2 [C-7], 42.6 [C-4], 36.3 [C-3], 31.8 [C-6], 24.3 [C-5], 17.3 [C-9], 17.2 [C-8], 8.9 [C-10]; IR (CH_2Cl_2) ν_{CO} 2092(m), 2077(m), 2047(s), 2032(vs), 2022(vs), 2002(s), 1973(w), 1950(w), 1944(w), 1893(w), 1657(ester) cm^{-1} . FAB mass spectrum : m/z (%) 670(4) (M-CO) $^+$; 642(23) (M-2CO) $^+$; 614(6) (M-3CO) $^+$; 586(10) (M-4CO) $^+$; 558(30) (M-5CO) $^+$; 530(38) (M-6CO) $^+$; 502(16) (M-7CO) $^+$; 474(5) (M-8CO) $^+$. Anal. Calcd. for $\text{C}_{25}\text{H}_{22}\text{O}_{10}\text{Co}_2\text{Mo}$: C, 43.13; H, 3.18. Found : C, 43.07; H, 3.11.

Preparation of $\text{CpMoCo}_2(\text{CO})_7(\text{P}(\text{OMe})_3)\text{CCO}_2$ menthyl, 37

A solution of 33 (0.184 g, 0.26 mmol) and trimethylphosphite (0.032 mL, 0.26 mmol) was stirred together in THF (20 mL) for 47 hours at room temperature. The reaction was monitored by TLC on Kieselgel (eluent, ether/hexane, 12/88) showing two spots: dark green 37, R_f 0.29; green 33, R_f 0.14. The solvent was removed and the resulting green oil separated by flash chromatography on silica gel (eluent, ether/hexane, 22/78). The product was obtained as a green oil, 37 (0.0836 g, 0.11 mmol, 42%).

^{31}P NMR (CD_2Cl_2) [300 K] 162.4 and 157.4 ppm. IR(CH_2Cl_2) ν_{CO} 2055(s), 2000(vs), 1990(sh), 1970(sh), 1920(m), 1865(m), 1655(ester) cm^{-1} . The FAB mass spectrum indicates the presence of a very small amount of disubstituted product. FAB mass spectrum: m/z (%) 797(12) ($\text{M}+1$) $^+$; 768(10) ($\text{M}-\text{CO}$) $^+$; 740(14) ($\text{M}-2\text{CO}$) $^+$; 712(44) ($\text{M}-3\text{CO}$) $^+$; 684(71) ($\text{M}-4\text{CO}$) $^+$; 656(19) ($\text{M}-5\text{CO}$) $^+$; 628(65) ($\text{M}-6\text{CO}$) $^+$; 600(25) ($\text{M}-7\text{CO}$) $^+$. $\text{CpMoCo}_2(\text{CO})_6(\text{P}(\text{OMe})_3)_2\text{CCO}_2\text{menthyl}$: FAB mass spectrum: m/z (%) 836(5) ($\text{M}-2\text{CO}$) $^+$; 808(7) ($\text{M}-3\text{CO}$) $^+$; 780(25) ($\text{M}-4\text{CO}$) $^+$; 752(4) ($\text{M}-5\text{CO}$) $^+$; 724(11) ($\text{M}-6\text{CO}$) $^+$.

Preparation of $\text{CpMoCo}_2(\text{CO})_7(\text{P}(\text{C}_6\text{H}_{11})_3)_2\text{CCO}_2\text{menthyl}$, 38

Tricyclohexylphosphine (0.0780 g, 0.28 mmol) and 33 (0.1825 g, 0.26 mmol) were stirred together in THF (20 mL) at ambient temperature for 38 hours. The progress of the reaction was monitored by TLC on Kieselgel (eluent, ether/hexane, 16/84) showing three spots: yellow-green, 38, R_f 0.65; UV visible, $\text{P}(\text{C}_6\text{H}_{11})_3$, R_f 0.40; dark green, 33, R_f 0.25. Flash chromatography on silica (eluent, ether/hexane, 7/93) was used to separate the product from the starting materials. A dark green solid 38, was obtained (0.1436 g, 0.15 mmol, 58%): mp 62-64°C; ^{31}P NMR (CD_2Cl_2) [300 K] 52.0 and 50.9 ppm. IR(CH_2Cl_2) ν_{CO} 2090(w), 2075(w), 2050(s), 2025(s), 2000(s), 1970(m), 1930(m), 1855(w), 1725(sh), 1645(ester) cm^{-1} . FAB mass spectrum: m/z (%)

896(5) (M-2CO)⁺; 840(8) (M-4CO)⁺; 784(71) (M-6CO)⁺;
 758(100) (M-7CO)⁺; 728(5) (M-5CO-C₆H₁₁)⁺; 702(89)
 (M-6CO-C₆H₁₁)⁺; 676(27) (M-7CO-C₆H₁₁)⁺; 648(38) (M-5CO-
 2C₆H₁₁)⁺. Anal. Calcd. for C₄₂H₅₇O₉Co₂MoP: C, 53.06;
 H, 6.04. Found: C, 52.94; H, 6.28.

Preparation of CpMoCo₂(CO)₇(PPh₃)CCO₂menthyl

Triphenylphosphine (0.076 g, 0.29 mmol) and 33 (0.209 g, 0.30 mmol) were stirred together in THF (20 mL) at room temperature for 48 h, at which point the development of the product was just barely visible as a light green spot (R_f 0.33) by TLC (eluent, ether/hexane, 15/85). Additional PPh₃ (0.011 g, 0.04 mmol) was added to the solution. The reaction was left to stir for 5 days. The product obtained was inseparable from the reactant cluster. ³¹P NMR (CH₂Cl₂) [300 K] 28.0 ppm.

Preparation of CpMoCo₂(CO)₇(P(OMe)₃)CCO₂exo-bornyl, 39

A solution of 34 (0.151 g, 0.22 mmol) and trimethylphosphite (0.25 mL, 2.1 mmol) was stirred in THF (25 mL) for 20 h at room temperature. The reaction was monitored by TLC (eluent, ether/hexane, 30/70) showing two products: dark green, R_f 0.24 and yellow-green, R_f 0.15. These products were separated by flash chromatography. A solution of 40 % CH₂Cl₂/hexane was used to elute the first

band, followed by a 25 % ether/ hexane solution, which removed the second band. FAB mass spectrometry identified the yellow-green product as the disubstituted cluster, 40. The monosubstituted product, 39, was present as the dark green band.

The product, 39, was obtained as a dark green solid (0.027 g, 0.03 mmol, 16 %). ^{31}P NMR (CH_2Cl_2) [300 K] 159 ppm [broad]. IR (CH_2Cl_2) ν_{CO} 2060(s), 2020(vs), 2010(vs), 1985(sh), 1930(m), 1871(m), 1660(ester) cm^{-1} . FAB mass spectrum : m/z (%) 794(3) (M^+); 738(18) ($\text{M}-2\text{CO}^+$); 710(48) ($\text{M}-3\text{CO}^+$); 682(100) ($\text{M}-4\text{CO}^+$); 654(14) ($\text{M}-5\text{CO}^+$); 626(52) ($\text{M}-6\text{CO}^+$); 598(11) ($\text{M}-7\text{CO}^+$). Anal. Calcd. for $\text{C}_{27}\text{H}_{31}\text{O}_{12}\text{Co}_2\text{MoP}$: C,40.93; H,3.94. Found : C,41.13; H,4.08.

The disubstituted product, 40, was obtained as a light green solid (0.046 g, 0.05 mmol, 24 %). ^{31}P NMR (CH_2Cl_2) [300 K] 156 ppm [broad]. IR (CH_2Cl_2) ν_{CO} 2040(s), 2005(vs), 1990(vs), 1965(sh), 1910(m), 1850(m), 1658(ester) cm^{-1} . FAB mass spectrum : m/z (%) 890(4) (M^+); 834(23) ($\text{M}-2\text{CO}^+$); 806(18) ($\text{M}-3\text{CO}^+$); 778(83) ($\text{M}-4\text{CO}^+$); 750(10) ($\text{M}-5\text{CO}^+$); 722(19) ($\text{M}-6\text{CO}^+$).

Preparation of $\text{CpMoCo}_2(\text{CO})_7(\text{P}(\text{C}_6\text{H}_{11})_3)\text{CCO}_2$ *exo*-bornyl

Tricyclohexylphosphine (0.088 g, 0.32 mmol) and 34 (0.183 g, 0.26 mmol) were stirred in THF (15 mL) at ambient

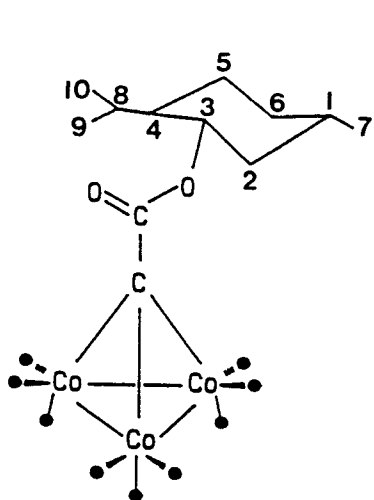
temperature for 22 h. The progress of the reaction was followed by TLC (eluent, ether/hexane, 20/80) showing the formation of the product as a yellow-green spot (R_f 0.79). Flash chromatography (eluent, ether/hexane, 10/90) was used to separate the product from the starting materials, yielding the phosphine substituted product as a green solid (0.057 g, 0.06 mmol, 23 %). ^{31}P NMR (CH_2Cl_2) [300 K] 55.1 and 56.2 ppm. IR (CH_2Cl_2) ν_{CO} 2085(w), 2077(w), 2048(w), 2030(s), 2028(s), 2002(vs), 1995(sh), 1960(m), 1945(w), 1925(w), 1657(ester, broad) cm^{-1} . FAB mass spectrum : m/z (%) 894(13) ($\text{M}-2\text{CO}$) $^+$; 866(5) ($\text{M}-3\text{CO}$) $^+$; 838(9) ($\text{M}-4\text{CO}$) $^+$; 782(20) ($\text{M}-6\text{CO}$) $^+$; 754(31) ($\text{M}-7\text{CO}$) $^+$. Anal. Calcd. for $\text{C}_{42}\text{H}_{55}\text{O}_9\text{Co}_2\text{MoP}$: C, 53.18; H, 5.84. Found : C, 52.92; H, 5.50.

Preparation of $\text{CpMoCo}_2(\text{CO})_7(\text{PPh}_3)\text{CCO}_2$ *exo-bornyl*

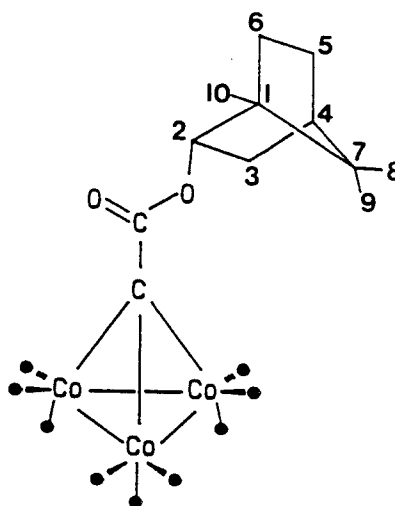
A solution of triphenylphosphine (0.066 g, 0.25 mmol) and the cluster 34 (0.092 g, 0.13 mmol) was stirred in THF (15 mL) at room temperature for 42 h. TLC on Kieselgel showed the formation of the product at R_f 0.22 as a faint green spot. It was not possible to separate the product from the cluster, 34. ^{31}P NMR (CH_2Cl_2) [300 K] 45.6 and 28.8 ppm. FAB mass spectrum : m/z (%) 848(13) ($\text{M}-3\text{CO}$) $^+$; 820(4) ($\text{M}-4\text{CO}$) $^+$; 792(100) ($\text{M}-5\text{CO}$) $^+$; as well as those peaks corresponding to the cluster 34.

5.4 Numbering system

NMR assignments are based on the following numbering scheme:



15



16

References

1. a) B. R. Penfold and B. H. Robinson, *Acc. Chem. Res.* (1973), 6, 73.
b) F. G. A. Stone, *Acc. Chem. Res.* (1981), 14, 318.
c) H. Vahrenkamp, *Adv. Organomet. Chem.* (1983), 22, 169.
2. N. N. Greenwood and A. Earnshaw, "Chemistry of the Elements", Pergamon Press, Oxford, England, 1986, p.1324.
3. F. A. Cotton and G. Wilkinson, "Advanced Inorganic Chemistry", John Wiley and Sons, New York, 1980, p.1081.
4. *ibid*, p.1082
5. R. Markby, J. Wender, R. A. Friedel, F. A. Cotton and H. W. Sternberg, *J. Am. Chem. Soc.*, (1958), 80, 6529.
6. P. W. Sutton and L. F. Dahl, *J. Am. Chem. Soc.*, (1967), 89, 261.
7. a) G. Bor, B. Marko and L. Marko, *Acta Chim. Acad. Sci. Hung.*, (1961), 27, 395.
b) W. T. Dent, L. A. Duncanson, R. G. Guy, H. W. B. Reed and B. L. Shaw, *Proc. Chem. Soc.*, London, (1961), 169.
8. D. Seyferth, J. E. Hallgren and P. L. K. Hung, *J. Organomet. Chem.*, (1973), 50, 265.
9. F. Bottomley and R. C. Burns, Eds., "Treatise on Dinitrogen Fixation", Wiley, 1979.

10. a) C. O'Connor and G. Wilkinson, *J. Chem. Soc. (A)*,
(1968), 2665.
b) R. L. Pruett, *Adv. Organomet. Chem.*, (1979), 17, 1.
11. N. N. Greenshaw and A. Earnshaw, "Chemistry of the
Elements", Pergamon Press, Oxford, England, 1986, p.1319.
12. P. M. Lausarot, G. A. Vaglio and M. Valle, *Inorg. Chim.
Acta*, (1977), 25, L107.
13. R. C. Ryan, C. U. Pittman Jr. and J. P. O'Connor,
J. Am. Chem. Soc., (1977), 99, 1986.
14. F. A. Cotton and G. Wilkinson, "Advanced Inorganic
Chemistry", John Wiley and Sons, New York, 1980, p.1289.
15. W. S. Knowles, *Acc. Chem. Res.*, (1983), 16, 106.
16. H. E. Howard-Lock and C. J. L. Lock, *Canadian Chemical
News*, (1987), 39, 7.
17. F. G. A. Stone, *Angew. Chem. Int. Ed. Engl.*, (1984),
23, 89.
18. H. Vahrenkamp, *Adv. Organomet. Chem.*, (1983), 22, 169.
19. C. U. Pittman Jr., M. G. Richmond, M. Absi-Halabi, F.
Richter and H. Vahrenkamp, *Angew. Chem. Int. Ed. Engl.*,
(1982), 21, 786.
20. K. A. Sutin, J. W. Kolis, M. Mlekuz, P. Bougeard, B. G.
Sayer, M. A. Quilliam, R. Faggiani, C. J. L. Lock, M. J.
McGlinchey and G. Jaouen, *Organometallics*, (1987), 6, 439.

21. D. T. Clark, K. A. Sutin, R.E. Perrier and M. J. McGlinchey, *Polyhedron*, in press.
22. R. Blumhofer and H. Vahrenkamp, *Chem. Ber.*, (1986), *119*, 683.
23. D. T. Clark, K. A. Sutin and M. J. McGlinchey, *Organometallics*, in press.
24. A. L. Lehninger, "Biochemistry", Worth Publishers, New York, 1977, p.296.
25. M. Mlekuz, P. Bougeard, M.J. McGlinchey and G. Jaouen, *J. Organomet. Chem.*, (1983), *253*, 117.
26. S. Jensen, B. H. Robinson and J. Simpson, *J. Chem. Soc., Chem. Commun.*, (1983), 1081.
27. G. Crane, C. E. Boord and A. L. Henne, *J. Am. Chem. Soc.*, (1945), *67*, 1237.
28. E. W. Abel, A. Singh and G. Wilkinson, *J. Chem. Soc.*, (1960), 1321.
29. R. B. King and M. B. Bisnette, *Inorg. Chem.* (1965), *4*, 475.
30. S. Aime, M. Botta, R. Gobetto, D. Osella and L. Milone, *Gazz. Chim. Italiana*, (1987), *117*, 773.
31. Chem-X, July 1986 version, developed and distributed by Chemical Design Ltd., Oxford, England.
32. I. W. Ramsey and D. Rogers, *Acta Cryst.*, (1952), *5*, 268.

33. A. Decken, D. T. Clark and M. J. McGlinchey, to be submitted for publication.
34. D. H. R. Barton and S. W. McCombie, *J. C. S. Perkin I*, (1975), 1574.
35. G. Mignani, H. Patin and R. Dabard, *J. Organomet. Chem.* (1979), 169.
36. R. Benn and H. Guenther, *Angew. Chem. Int. Ed. Engl.* (1983), 22, 350.
37. T. W. Matheson, B. H. Robinson and W. S. Tham, *J. Chem. Soc. (A)*, (1971), 1457.
38. N. N. Greenwood and A. Earnshaw, "Chemistry of the Elements", Pergamon Press, Oxford, England, 1986, p.566.
39. T. W. Matheson and B. R. Penfold, *Acta Cryst., Sect. B*, (1977), B33(6), 1980.
40. S. Aime, M. Botta, R. Gobetto and D. Osella, *J. Organomet.Chem.*, (1987), 320, 229.
41. J. G. Smith and G.F. Wright, *J. Org. Chem.*, (1952), 17, 1116.
42. R. T. Markham, E. A. Dietz Jr. and D. R. Martin, *Inorganic Synthesis*, (1976), 16, 161.
43. J. D. Morrison and W. F. Masler, *J. Org. Chem.*, (1974), 39, 270.
44. K. Malisza, K. A. Sutin, R. E. Perrier and M. J. McGlinchey, work in progress.

45. D. D. Perrin and D.R. Perrin, "Purification of Laboratory Chemicals", Pergamon Press, New York, 1980.